Performance Analysis of Multi-Cell Full-duplex Cellular Networks

IEEE Access
Multidisciplinary ⋮ Rapid Review ⋮ Open Access Journal

Date of publication xxxx 00, 0000, date of current version xxxx 00, 0000.

Digital Object Identifier xxxxx.DOI

Performance Analysis of Multi-Cell Full-duplex Cellular Networks

HUASEN HE[1] (Member, IEEE), SUDIP BISWAS[2], PAULA AQUILINA[3], THARMALINGAM RATNARAJAH[3] (Senior Member, IEEE), JIAN YANG[1] (Senior Member, IEEE)

[1]Department of Automation, School of Information Science and Technology, Univ. of Science and Technology of China, Hefei, 230027, Anhui, China (e-mail: hehuasen@ustc.edu.cn, jianyang@ustc.edu.cn)
[2]Department of Electronics and Communications Engineering, Indian Institute of Information Technology Guwahati (IIITG), Guwahati, India.(e-mail: sudip.biswas@ieee.org)
[3]Institute for Digital Communications (IDCOM), School of Engineering, The University of Edinburgh, Edinburgh, UK.(e-mail: aquilinapaula@gmail.com, T.Ratnarajah@ed.ac.uk)

Corresponding author: Jian Yang (e-mail: jianyang@ustc.edu.cn).

This work was supported in part by Anhui Provincial Natural Science Foundation under Grant 1908085QF266, in part by the Strategic Priority Research Program of the Chinese Academy of Sciences under Grant ZDRW-KT-2016-02, in part by Youth Innovation Promotion Association of the Chinese Academy of Sciences under Grant CX2100107001, in part by the China Electronics Technology Group Corporation (CETC) Joint Advanced Research Foundation under Grant 6141B08080101, and in part by the UK Engineering and Physical Sciences Research Council (EPSRC) under Grant EP/P009549/1.

ABSTRACT We analyze the performance of a cellular network, where Poisson point process distributed half-duplex (HD) downlink (DL) and uplink (UL) users are served by multiple full-duplex (FD) base stations (BSs). To address the surge in interference in the network due to the simultaneous operation in time and frequency of the FD BSs, we (a) adopt a self-interference cancellation scheme at each BS, and (b) apply linear interference alignment in each cell to cancel the intra-cell interference. Further, to better capture the distribution of the FD BSs, we model the BSs as a Matérn hard-core point process, in which a minimum distance is imposed between points. The performance of both UL and DL users is analyzed by deriving general expressions and closed-form approximations for the outage probability and throughput. Next, simulations are carried out for both macro and micro cell environments under both FD and HD operations with respect to various network parameters. Our results reveal several fundamental characteristics and the necessary conditions required for the successful deployment of such networks.

INDEX TERMS Full-duplex Communication, Interference Alignment, Matérn Hard-core Point Process, Stochastic Geometry.

I. INTRODUCTION

FULL-DUPLEX (FD) wireless communication, which caters for simultaneous transmission and reception at the same time-frequency band, has attracted a great deal of attention for its potential to double the spectrum efficiency and reduce end-to-end latency when compared to half-duplex (HD) systems. However, the primary predicament of FD systems is the strong self-interference (SI), whereby the transmitted power interferes with the uplink (UL) received signals at the FD nodes [1]–[3]. This issue can be tackled primarily in the propagation domain, where the aim is to limit the amount of SI as much as possible. This can be achieved via the use of directional antennas and antenna separation methods (both in terms of distance and via the use of RF absorbers) [4]. However, such techniques on their own do not suppress the SI to a level that is suitable for communication. Thanks to some recent breakthroughs in analog and digital domain SI cancellation techniques [5], [6], that have allowed to suppress the SI below the noise floor level and make FD communication a true possibility.

However, SI is not the only challenge in realizing a FD wireless network. In particular, in a multi-cell FD wireless network, all transceivers operate at the same time and frequency, implying that receivers are susceptible to interference from every transmitter. The resulting intra-cell and inter-cell interference can cause significant performance degradation in such networks. Therefore, to implement FD operation in practice, it is fundamental to find appropriate techniques to manage the intra-cell and inter-cell interferences.

Some noteworthy developments in this direction can be found in recent literature with the objective of reducing interference and analyzing the performance of FD enabled

networks. In the following subsection, we mention a few references, which although by no means is exhaustive, fairly indicate the scope and trend of research on FD networks.

1) Related literature

The study on FD communication spans over various system configurations and network topologies in literature. For example, the use of FD communication in cognitive radio networks makes it possible for the secondary users to sense spectrum and transmit at the same time. The spectrum sensing approaches and security requirements for FD cognitive radio networks were summarized in [7], while the motivations and challenges of FD cognitive radio networks were also provided. The outage performance and diversity gain of multirelay systems were analyzed in [8], which proved the high spectrum efficiency of FD multirelay channels. For both two-node and three-node FD architectures, authors in [9] shown that employing directional antennas can significantly reduce the loopback interference. The potential FD techniques including SI cancellation, MAC layer protocol design and relay selection were reviewed and summarized in [10], [11], while [11] provided a survey of in-band FD transmission, which reviewed the existing works on the physical layer performance of in-band FD systems. According to [11], FD network topologies can be generally categorized into three types including bi-directional, relay and cellular topology networks. The bi-directional topology consists of pair FD nodes which transmit and receive signals at the same time and frequency. It has been shown that the bi-directional topology networks have the potential to double the spectrum efficiency over that of HD networks [12], [13]. In FD relay networks, the end-to-end latency can be reduced as a relay node can receive data from a source node and transmit data to a destination node simultaneously within all the same frequency band [11], [14]. As for cellular topology, which is the focus of this paper, BSs or users are capable of FD transmission and BSs can serve DL and UL users in the same frequency band. The spectrum efficiency and power efficiency of single-cell and multi-cell FD networks were studied in [15], where power control and user scheduling were adopted. The up- and downlink ergodic achievable rates of a a multi-cell multi-user MIMO full-duplex network were studied in [16], where both FD and HD users were considered and linear precoders and receivers were adopted. To mitigate inter-cell interference in FD ultra-dense small cell networks, a resource split approach was proposed in [17], which classified BS into two groups and allocated half of the resources to each group. The system-level performance of FD MIMO cellular networks was analyzed in [18] while [19] optimized the throughput of a FD wireless network with various transmission strategies. For heterogeneous networks, the interference from cells operating in FD mode was studied in [20], where the throughput of a hybrid FD/HD multi-tier heterogeneous network was derived.

In the studies reported above (i.e. [15]–[20]), it was assumed that BSs are randomly located which means that BSs can be very close to each other. Applying this assumption to the location of BSs may be inaccurate and inconsistent with the actual scenario, where in practice the locations of BSs are carefully planned. Moreover, inter-cell interference from BSs caused significant performance degradation in UL transmission and it was reported in [18] that sufficient spacing between FD BSs in microcells is necessary to make UL transmission feasible. Therefore, in this paper, we adopt a more general and realistic scenario where BSs are distributed according to a Martérn Hard-core point process (HCPP) [21]. In HCPP, a minimum distance, also referred to as the hard-core distance, is imposed between points. It was shown in [22] that HCPP is more accurate than Poisson point process (PPP) when modeling the locations of BSs in real cellular networks obtained from a public database. By setting a hard-core distance and modeling the locations of BSs as a HCPP, it is possible to suppress the inter-cell interference from BSs.

For networks equipped with FD BSs, DL users suffer from additional co-channel interference (CCI) from UL users within the same cell. Since these interferers are from the same cell, distances are short and the power at which they are received is quite significant. Therefore, particular attention must be paid to the management of intra-cell interference for the practical implementation of FD networks. A highly promising technique that can be used to manage intra-cell interference is interference alignment (IA), initially proposed in [23]. Due to its potential to approach the Shannon capacity of interference networks in the high Signal-to-Noise Ratio (SNR) regime, IA has been widely studied in literature. In [24], a distributed numerical IA approach was proposed for HD interference channels, where only local channel state information (CSI) at each node was required to perform minimum weighted leakage interference (Min-WLI) and maximum signal-to-interference-plus-noise ratio (Max-SINR) based IA. Further, in [25] a minimum mean square error (MMSE) based IA algorithm was also proposed for the HD IC. Similarly, for FD systems, while the degrees of freedom (DoF) region was derived in [26], the feasibility of linear IA was studied in [27]. Both the Max-SINR and MMSE based IA algorithms were used to develop beamformers for FD multi-cell networks in [28]. Further, consider a M-cell network, the scalability of FD's multiplexing gain was characterized and analyzed in [29], where IA was adopted to mitigate the uplink-downlink interference. However, the work in [24]–[29] either considered fixed network settings or ignored the impacts of path loss. Accordingly, in this paper we leverage the analysis of [28] and use linear IA to manage interference in FD networks.

2) Contribution of this paper

There have been few works (e.g. [30]–[33]) investigating HCPP in FD networks. In [31], [32], HCPP was used in simulations to model the locations of BSs, and its statistic characteristics were not leveraged in performance analysis of FD networks. In [30], BSs serving one user each were assumed to distributed according to a PPP while only a

subset of BSs which transmit in the same frequency band was modeled as a HCPP. In [33], a fixed number of DL users was considered, and only the capacity of users was analyzed. To the best of the author's knowledge, this paper is the first to study the performance of a general and realistic FD cellular network where FD BSs are modeled as a HCPP while DL and UL HD users are distributed according to PPPs. Both UL and DL performances are analyzed in terms of outage probability, throughput and ergodic capacity, while closed-form approximations for outage probability and throughput are also provided in this work. Monte Carlo simulations are used to verify the analytical results. The main distinctions and findings of this work are summarized below.

- In contrast to previous works that model the spatial distribution of BSs as a PPP, we adopt a more realistic HCPP model by imposing a hard-core distance between FD BSs, which helps to reduce inter-cell interference. Additionally, we use linear IA to cancel out the intra-cell interference from UL users towards DL users. The performance of both UL and DL transmissions are studied and closed-form approximations for outage probability and throughput are derived.
- The analytical and simulations results show that FD communication is always feasible in micro-cellular networks, while for the case of macro-cellular networks, large hard-core distances between the BSs are required to make the UL transmission possible.
- For micro-cellular networks, our results show that interference from neighboring BSs has the most significant impact on system performance, while residual SI can be ignored due to the low transmit power. By applying linear IA and modeling the BS locations as an HCPP, FD networks can provide better performance than HD networks in terms of user capacity and the ratio of UL user capacity in FD networks to that in HD networks increases with the hard-core distance. Moreover, we show that when the hard-core distance is greater than the critical distance, the UL transmission in FD networks has the potential to double the spectrum efficiency.
- For scenarios where BSs have a limited number of transmit antennas, only a limited number of users can be served. Our results show that it can be assumed that all users can be served when the maximum numbers of DL and UL users (which satisfy the IA feasibility conditions) are equal to or greater than twice the mean numbers of PPP distributed DL and UL users in each cell. Moreover, we show that UL user performance can be improved by increasing the maximum number of UL users which satisfies the IA feasibility conditions, while in low and high targeted SINR regime, reducing the maximum number of DL users served by each BS has limited impact on UL performance.
- Finally, compared to PPP-based model, the inter-cell interference can be suppressed by increasing the hard-core distance between BSs. In particular, DL transmission can be improved when utilizing FD BSs, while UL transmission can outperform conventional HD networks when the hard-core distance is greater than a specific threshold.

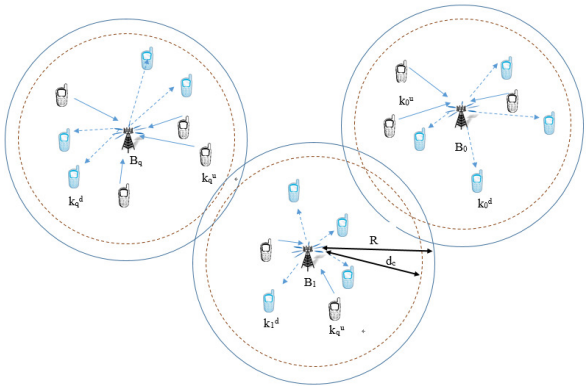

FIGURE 1: System model of a multiple cell network with FD BSs and HD users.

3) Notations

Throughout the paper, matrices and vectors are denoted by bold uppercase and bold lowercase letters, respectively. We will use B_q to represent the qth BS and k_q^d (k_q^u) to denote the kth DL(UL) user served by the qth BS. Circularly symmetric complex Gaussian distribution with mean μ and variance τ^2 is denoted as $\mathcal{CN}(\mu, \tau^2)$, while $\mathcal{U}[n, m]$ represents uniform distribution between n and m. Transpose operator of a matrix is denoted as $(\cdot)^T$ and $\det(\cdot)$ is the determinant of a matrix. Expectation operation and natural logarithm are represented by $\mathbb{E}[\cdot]$ and $\ln(\cdot)$. Finally, $\mathbb{C}^{n\times m}$ is used to represent the set of $n \times m$ complex matrices.

II. SYSTEM MODEL

We consider a similar setting in [33], where the locations of multiple FD BSs are modeled as a HCPP Φ_M with intensity λ_M and hard-core distance d_c. As shown in Fig.1, each BS is equipped with M_d transmit antennas and M_u receive antennas to serve multiple DL and UL HD users in circular regions with radius R, centered around the BSs. Defer from [33], for each BS the associated DL and UL users are randomly distributed in the circular region according to PPP with intensities λ_P^d and λ_P^u respectively [34]. Furthermore, DL users, requiring b_d streams each, are equipped with N_d antennas; while UL users, requiring b_u streams each, are equipped with N_u antennas.

Without loss of generality, we consider that a typical BS denoted as B_0 and its associated DL and UL users are in φ_0 and ϕ_0, respectively. All UL and DL users are assumed to be randomly ordered. BS antennas have a gain of G_b, while user antennas are unit-gain. The signal received at the kth DL user

and the UL signal seen at B_0 are respectively given as

$$\boldsymbol{s}_{k_0^d} = \sum_{i_0^d \in \varphi_0} \sqrt{\frac{G_b \beta}{l^{\alpha}_{k_0^d, B_0}}} \boldsymbol{H}_{k_0^d, B_0} \boldsymbol{V}_{i_0^d} \boldsymbol{s}_{i_0^d} + \sum_{j_0^u \in \phi_0} \sqrt{\frac{\beta_u}{l^{\alpha_u}_{k_0^d, j_0^u}}} \boldsymbol{H}_{k_0^d, j_0^u} \boldsymbol{V}_{j_0^u} \boldsymbol{s}_{j_0^u} + \sum_{B_q \in \Phi_M q \neq 0} \left(\sum_{i_q^d \in \varphi_q} \sqrt{G_b \beta l^{-\alpha}_{k_0^d, B_q}} \boldsymbol{H}_{k_0^d, B_q} \boldsymbol{V}_{i_q^d} \boldsymbol{s}_{i_q^d} + \sum_{j_q^u \in \phi_q} \sqrt{\beta_u l^{-\alpha_u}_{k_0^d, j_q^u}} \boldsymbol{H}_{k_0^d, j_q^u} \boldsymbol{V}_{j_q^u} \boldsymbol{s}_{j_q^u} \right) + \boldsymbol{n}_{k_0^d}, \tag{1}$$

$$\boldsymbol{s}_{k_0^u} = \sum_{j_0^u \in \phi_0} \sqrt{\frac{G_b \beta}{l^{\alpha}_{B_0, j_0^u}}} \boldsymbol{H}_{B_0, j_0^u} \boldsymbol{V}_{j_0^u} \boldsymbol{s}_{j_0^u} + \sum_{i_0^d \in \varphi_0} \sqrt{G_b^2 \beta_b} \boldsymbol{H}_{B_0, B_0} \boldsymbol{V}_{i_0^d} \boldsymbol{s}_{i_0^d} + \sum_{B_q \in \Phi_M q \neq 0} \left(\sum_{i_q^d \in \varphi_q} \sqrt{G_b^2 \beta_b l^{-\alpha_b}_{B_0, B_q}} \boldsymbol{H}_{B_0, B_q} \boldsymbol{V}_{i_q^d} \boldsymbol{s}_{i_q^d} + \sum_{j_q^u \in \phi_q} \sqrt{G_b \beta l^{-\alpha}_{B_0, j_q^u}} \boldsymbol{H}_{B_0, j_q^u} \boldsymbol{V}_{j_q^u} \boldsymbol{s}_{j_q^u} \right) + \boldsymbol{n}_{B_0}. \tag{2}$$

Here, $l_{k_q^d, B_0}$ and l_{B_0, j_q^u}, denote the distance from B_0 to the kth DL user and the jth UL user associated with BS B_q, respectively. Due to the random locations of UL and DL users, the probability density functions (PDFs) of $l_{k_0^d, B_0}$ and l_{B_0, j_0^u} can be written as

$$f_{l_{k_0^d, B_0}}(r) = f_{l_{B_0, j_0^u}}(r) = \frac{2r}{R^2}. \tag{3}$$

We use $l_{k_0^d, j_q^u}$ to represent the distance from DL user k_0^d to UL user j_q^u, and the distance from BS B_q to B_0 is expressed as l_{B_0, B_q}. The path loss intercepts of BS-user, user-user and BS-BS are denoted as β, β_u and β_b respectively, while α, α_u and α_b are the corresponding path loss exponents. Since a multi-slope model can better capture the pathloss among BSs when compared with a single slope model [18], [35], we adopt a two-slope pathloss model for the BS-BS link. For a given distance l_{B_0, B_q}, we have [33], [35]

$$\begin{cases} \beta_b = \beta_{b_1}, \alpha_b = \alpha_{b_1} & l_{B_0, B_q} \leq R_c \\ \beta_b = \beta_{b_2}, \alpha_b = \alpha_{b_2} & l_{B_0, B_q} > R_c \end{cases} \tag{4}$$

where $R_c = 4h_{BS}^2/\xi$ is the critical distance, h_{BS} is the BS antenna height and ξ is the wavelength. $\boldsymbol{H}_{i_0^d, B_q} \in \mathbb{C}^{N_d \times M_d}$ represents the channel from BS B_q to DL user i_0^d, and the channel between the jth UL user communicated with BS B_q and user i_0^d is denoted as $\boldsymbol{H}_{i_0^d, j_q^u} \in \mathbb{C}^{N_d \times N_u}$. The channel between BSs B_0 and B_q is represented as $\boldsymbol{H}_{B_0, B_q} \in \mathbb{C}^{M_u \times M_d}$, while SI channel at B_0 is denoted as $\boldsymbol{H}_{B_0, B_0} \in \mathbb{C}^{M_u \times M_d}$. According to [18], small scale fading between BSs can be modelled as Rayleigh, Rician or disregarded. To keep consistent with BS-user, user-BS and user-user links, we adopt Rayleigh fading for BS-BS links [36]. It is assumed that all channel matrix elements are independent and identically distributed (i.i.d.) complex normal random variables with zero mean and variance one. Moreover, $\boldsymbol{s}_{i_q^d} \in \mathbb{C}^{b_d \times 1}$ is the data intend for the ith DL user associated with BS B_q, with $\mathbb{E}\{\boldsymbol{s}_{i_q^d} \boldsymbol{s}_{i_q^d}^H\} = P_d \boldsymbol{I}$; while $\boldsymbol{s}_{j_q^u}$ represents the transmitted data intended for UL user j_q^u, with $\mathbb{E}\{\boldsymbol{s}_{j_q^u} \boldsymbol{s}_{j_q^u}^H\} = P_u \boldsymbol{I}$. The precoders for $\boldsymbol{s}_{i_q^d}$ and $\boldsymbol{s}_{j_q^u}$ are $\boldsymbol{V}_{i_q^d} \in \mathbb{C}^{M_d \times b_d}$ and $\boldsymbol{V}_{j_q^u} \in \mathbb{C}^{N_u \times b_u}$, respectively. Finally, $\boldsymbol{n}_{i_0^d}$ and $\boldsymbol{n}_{B_0}$ represent additive white Gaussian noise (AWGN) seen at the DL users and the BSs respectively, and both have zero mean and variance $\sigma^2 \boldsymbol{I}$.

Since each BS only serves DL and UL users in its own cell, it is reasonable to assume that perfect CSI is shared between a BS and its associated users. The CSI for the link from the UL users to the DL users can be obtained by measuring the pilot signals from UL users, and then the DL users transmit the CSI to BSs. Unlike other IA related works (e.g. [23], [25]–[28]) where global CSI was assumed, in this work we use only CSI within the cell to keep CSI overheads within acceptable limits. Therefore, intra-cell interference can be eliminated by adopting linear IA techniques. Assuming $\boldsymbol{U}_{k_0^d} \in \mathbb{C}^{N_d \times b_d}$ is the unitary receive beamformer applied at DL user k_0^d and $\boldsymbol{U}_{k_0^u} \in \mathbb{C}^{N_u \times b_u}$ is the unitary receiver applied at B_0 to extract the data from UL user k_0^u, the feasibility conditions for IA to eliminate intra-cell interference are given by [27]

$$| \boldsymbol{u}_{k_0^d, t}^H \boldsymbol{H}_{k_0^d, B_0} \boldsymbol{v}_{k_0^d, t} | > 0 \quad \forall k, t \tag{5a}$$

$$| \boldsymbol{u}_{k_0^u, t}^H \boldsymbol{H}_{B_0, k_0^u} \boldsymbol{v}_{k_0^u, t} | > 0 \quad \forall k, t \tag{5b}$$

$$\boldsymbol{u}_{k_0^d, t}^H \boldsymbol{H}_{k_0^d, B_0} \boldsymbol{v}_{i_0^d, j} = 0 \quad \forall k, t, i, j, (k, t \neq i, j) \tag{5c}$$

$$\boldsymbol{u}_{k_0^u, t}^H \boldsymbol{H}_{B_0, k_0^u} \boldsymbol{v}_{i_0^u, j} = 0 \quad \forall k, t, i, j, (k, t \neq i, j) \tag{5d}$$

$$\boldsymbol{u}_{k_0^d, t}^H \boldsymbol{H}_{k_0^d, i_0^u} \boldsymbol{v}_{i_0^u, j} = 0 \quad \forall k, t, i, j\,. \tag{5e}$$

Here, $\boldsymbol{u}_{k_0^d, t}$, $\boldsymbol{u}_{k_0^u, t}$, $\boldsymbol{v}_{k_0^d, t}$ and $\boldsymbol{v}_{k_0^u, t}$ are the tth column of the beamformers $\boldsymbol{U}_{k_0^d}$, $\boldsymbol{U}_{k_0^u}$, $\boldsymbol{V}_{k_0^d}$ and $\boldsymbol{V}_{k_0^u}$ respectively. IA techniques designed for a single-cell with a FD BS serving multiple HD UL and DL users are already available in the literature, with both the MMSE based design (Algorithm 1 in [28]) and Max-SINR based technique (Algorithm 2 in [28]) being suited to our scenario. Using any of the two iterative techniques from [28] to design both precoders and decoders would achieve the IA conditions in (5) for the scenario outlined in this paper. For illustration, Fig. 2 shows the performance comparison between the FD-Max-SINR and FD-MMSE algorithms for a system with 2 FD BSs, 2 DL and 2 UL users associated with each BS and $b_d = b_u = 2$ with respect to varying antenna number pairs[1]. From the figure it can be seen that while both algorithms show similar sum rate performance, the processing time required for max-SINR algorithm is more than that of the MMSE based one due to its lower computational complexity. Hence, without loss of generality, in this paper we consider the MMSE based design from [28] for our analysis.

Further, Fig. 2.a also illustrates the IA feasibility conditions with respect to the number of antennas at the BSs and

[1]Fig. 2 has been generated by simulating the algorithms proposed in [28] in a centralized manner over 500 Monte Carlo iterations in MATLAB R20017a on a Windows 10 Pro PC (Intel i5-8300 processor (4 cores, each clocked at 2.30 GHz), 8 GB of memory and 8 GB of AMD Radeon RX 570 graphics memory).

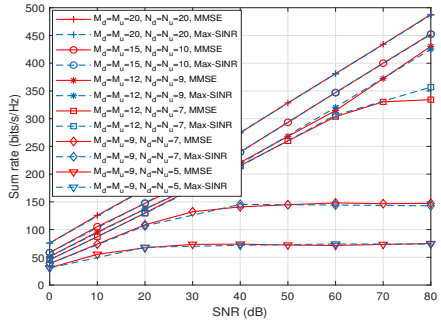

(a) Sum rate comparison

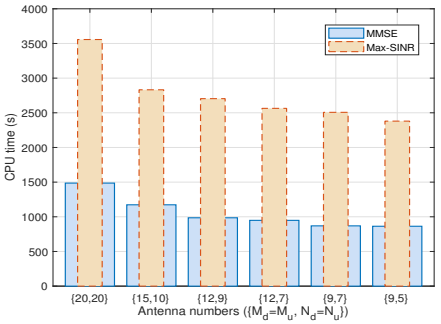

(b) Processing time comparison

FIGURE 2: Comparison between FD MMSE and FD Max-SINR IA algorithms.

users. In particular, for the antenna pairs $\{M_d = M_u,\, N_d = N_u\} = \{20, 20\}, \{15, 10\}, \{12, 9\}$, the curves have the same slope and the network achieves full DoF. However for $\{M_d = M_u,\, N_d = N_u\} = \{12, 7\}, \{9, 7\}, \{9, 5\}$, the sum rates attenuate with increasing SNR, which indicate that IA is infeasible. At this point, it is worth noting that since the UL users in this paper are modelled as a PPP, the number of UL users in a cell is a Poisson random variable (RV). Therefore, to meet the feasibility conditions of IA, we consider two different scenarios as mentioned below.

- **Scenario I:** The number of antennas at each BS is assumed to be large enough so that the feasibility conditions of IA can always be met, regardless of the number of DL and UL users, required streams and the number of antennas at the users.
- **Scenario II:** In this case, we assume only a limited number of antennas is available at each BS. Given the number of available antennas (at both BS and users) and the amount of data streams required at each DL and UL user, for IA to be feasible within each cell, only K_d^{max} out of a total K_d DL users and K_u^{max} out of a total K_u UL users can be served by each BS. Note that K_d^{max} and K_u^{max} are the maximum numbers of DL and UL users that can served by each BS in order for IA to be feasible within the cell. Its value can be obtained from the IA feasibility study in [27]. Since the transmit power of BS is higher than that of user, we assume the K_d^{max} served DL users are randomly selected. The K_u^{max} users selected to be served are those nearest to the BS, and signals from the rest of the $K_u - K_u^{max}$ UL users are treated as residual intra-cell interference.

Moreover, it can be reasonably assumed that an interference cancellation scheme (i.e. analog/digital cancellation) is used at each FD BSs to mitigate the effects of SI on system performance. Since an interference cancellation scheme is adopted at the BSs to mitigate the effects of SI, the strong line-of-sight component in SI can be estimated and removed similar to [4]. Additionally, a specific power value can be used to model the effect of the implementation of analog/digital SI cancellation, and represent the amount of residual SI left [37]. Thus, we model the entries of the residual SI channel as i.i.d. complex normal RVs with zero mean and variance σ_s^2. Using IA to cancel out intra-cell interference and applying the SI cancellation schemes to mitigate the effect of SI, the estimated signals can be written as

$$\begin{aligned}\hat{\boldsymbol{s}}_{k_0^d} &= \sqrt{G_b \beta l_{k_0^d, B_0}^{-\alpha}}\, \boldsymbol{U}_{k_0^d}^H \boldsymbol{H}_{k_0^d, B_0} \boldsymbol{V}_{k_0^d} \boldsymbol{s}_{k_0^d} \\ &+ \delta \sum\nolimits_{j_0^u \in \phi_0'} \sqrt{\beta_u l_{k_0^d, j_0^u}^{-\alpha_u}}\, \boldsymbol{U}_{k_0^d}^H \boldsymbol{H}_{k_0^d, j_0^u} \boldsymbol{V}_{j_0^u} \boldsymbol{s}_{j_0^u} \\ &+ \sum_{B_q \in \Phi_M q \neq 0} \boldsymbol{U}_{k_0^d}^H \left(\sum_{i_q^d \in \tilde{\varphi}_q} \sqrt{G_b \beta l_{k_0^d, B_q}^{-\alpha}}\, \boldsymbol{H}_{k_0^d, B_q} \boldsymbol{V}_{i_q^d} \boldsymbol{s}_{i_q^d} \right. \\ &\left. + \sum_{j_q^u \in \phi_q} \sqrt{\beta_u l_{k_0^d, j_q^u}^{-\alpha_u}}\, \boldsymbol{H}_{k_0^d, j_q^u} \boldsymbol{V}_{j_q^u} \boldsymbol{s}_{j_q^u} \right) + \boldsymbol{U}_{k_0^d}^H \boldsymbol{n}_{k_0^d}, \end{aligned} \tag{6}$$

$$\begin{aligned}\hat{\boldsymbol{s}}_{k_0^u} &= \\ &\sqrt{\frac{G_b \beta}{l_{B_0, k_0^u}^{-\alpha}}}\, \boldsymbol{U}_{k_0^u}^H \boldsymbol{H}_{B_0, k_0^u} \boldsymbol{V}_{k_0^u} \boldsymbol{s}_{k_0^u} + \sum_{i_0^d \in \tilde{\varphi}_0} \sqrt{G_b^2 \beta_b}\, \boldsymbol{U}_{k_0^u}^H \hat{\boldsymbol{H}}_{B_0, B_0} \boldsymbol{V}_{i_0^d} \boldsymbol{s}_{i_0^d} \\ &+ \delta \sum_{j_q^u \in \phi_0'} \sqrt{G_b \beta l_{B_0, j_0^u}^{-\alpha}}\, \boldsymbol{U}_{k_0^u}^H \boldsymbol{H}_{B_0, j_0^u} \boldsymbol{V}_{j_0^u} \boldsymbol{s}_{j_0^u} \\ &+ \sum_{B_q \in \Phi_M q \neq 0} \boldsymbol{U}_{k_0^u}^H \left(\sum_{i_q^d \in \tilde{\varphi}_q} \sqrt{G_b^2 \beta_b l_{B_0, B_q}^{-\alpha_b}}\, \boldsymbol{H}_{B_0, B_q} \boldsymbol{V}_{i_q^d} \boldsymbol{s}_{i_q^d} \right. \\ &\left. + \sum_{j_q^u \in \phi_q} \sqrt{G_b \beta l_{B_0, j_q^u}^{-\alpha}}\, \boldsymbol{U}_{k_0^u}^H \boldsymbol{H}_{B_0, j_q^u} \boldsymbol{V}_{j_q^u} \boldsymbol{s}_{j_q^u} \right) + \boldsymbol{U}_{k_0^u}^H \boldsymbol{n}_{B_0}, \end{aligned} \tag{7}$$

where $\tilde{\varphi}_q = (1-\delta)\varphi_q + \delta\varphi_q'$ and φ_q' is the subset of served DL users. ϕ_0' is the subset of ϕ_0 except for the K_u^{max} nearest UL users and $\hat{\boldsymbol{H}}_{B_0, B_0}$ represents the residual SI channel, with the elements of $\hat{\boldsymbol{H}}_{B_0, B_0}$ being i.i.d. $\mathcal{CN}(0, \sigma_s^2)$. For case I $\delta = 0$, while $\delta = 1$ in case II.

III. PRELIMINARIES

In this section, we provide some mathematical preliminaries which will be used in this paper.

A. DISTRIBUTIONS OF CHANNEL SQUARED NORMS

Assuming single-stream decoding is performed at DL users and BSs, the distributions of channel squared norms are provided in following lemma.

Lemma 1. *For the channel between a ($a \in \{B_0, k_0^d\}$) and b ($b \in \{B_q, i_q^u\}$ and $q \neq 0$), we have $2\times \parallel \boldsymbol{u}_{k_0^y,t}^H \boldsymbol{H}_{a,b} \boldsymbol{V}_{i_q^y} \parallel^2$ ($y \in \{d,u\}$) is a Chi-squared distributed RV with $2b_y$ degrees of freedom (DoF). The PDF of $\parallel \boldsymbol{u}_{k_0^y,t}^H \boldsymbol{H}_{a,b} \boldsymbol{V}_{i_q^y} \parallel^2$ can be expressed as*

$$f_{\chi^2}(2x; 2b_y) = \frac{x^{b_y-1}}{2\Gamma(b_y)} e^{-x} \qquad y \in \{d,u\}. \tag{8}$$

Especially, when $q = 0$ and $k = i$, we have $\parallel \boldsymbol{u}_{k_0^d,t}^H \boldsymbol{H}_{k_0^d,B_0} \boldsymbol{V}_{k_0^d} \parallel^2$ and $\parallel \boldsymbol{u}_{i_0^u,t}^H \boldsymbol{H}_{B_0,i_0^u} \boldsymbol{V}_{i_0^u} \parallel^2$ are exponentially distributed RVs with unit mean.

Proof. Since all columns of $\boldsymbol{U}_{k_0^y}$ and $\boldsymbol{V}_{i_q^y}$ have unit norm, $\boldsymbol{u}_{k_0^y,t}$ and $\boldsymbol{V}_{i_q^y}$ have no impact on the signal distribution. Moreover, all entries of $\boldsymbol{H}_{a,b}$ are complex Gaussian distributed RVs and $rank\{\boldsymbol{U}_{k_0^y} \boldsymbol{H}_{a,b} \boldsymbol{V}_{i_q^y}\} = b_y$ when $q \neq 0$. Thus, $2\times \parallel \boldsymbol{u}_{k_0^y,t}^H \boldsymbol{H}_{a,b} \boldsymbol{V}_{i_q^y} \parallel^2$ is a Chi-squared distributed RV with $2b_y$ DoF. When $q = 0$ and $k = i$, applying the IA conditions we have $\parallel \boldsymbol{u}_{k_0^y,t}^H \boldsymbol{H}_{a,b} \boldsymbol{V}_{k_0^y} \parallel^2 = \parallel \boldsymbol{u}_{k_0^y,t}^H \boldsymbol{H}_{a,b} \boldsymbol{v}_{k_0^y,t} \parallel^2$. Thus, $\parallel \boldsymbol{u}_{k_0^y,t}^H \boldsymbol{H}_{a,b} \boldsymbol{V}_{k_0^y} \parallel^2$ is Chi-squared distributed with 2 DoF (i.e. exponentially distributed with unit mean). □

B. A USEFUL LEMMA FOR CAPACITY ANALYSIS

To analyse the capacity of fading interference channel, a useful lemma is introduced in this subsection.

Lemma 2. *For arbitrary non-negative random variables $\{x_i | i = 1, 2, ..., N\}$ and $\{y_j | j = 1, 2, ..., M\}$, the following equation can be obtained [38]*

$$\mathbb{E}\left[\ln\left(1 + \frac{\sum_{i=1}^N x_i}{\sum_{j=1}^M y_j + 1}\right)\right] = \int_0^\infty \frac{\mathcal{M}_y(z) - \mathcal{M}_{x,y}(z)}{z} e^{-z} dz \tag{9}$$

where $\mathcal{M}_y(z) = \mathbb{E}\left[e^{-z\sum_{j=1}^M y_j}\right]$ and $\mathcal{M}_{x,y}(z) = \mathbb{E}\left[e^{-z\left(\sum_{i=1}^N x_i + \sum_{j=1}^M y_j\right)}\right]$.

IV. PERFORMANCE ANALYSIS

A. PERFORMANCE OF A GENERIC DL USER SERVED BY FD BSS

1) Outage probability for each data stream of a generic DL user

Assuming all DL users perform single-stream decoding as in [39], the tth data stream of DL user k_0^d is given by

$$\begin{aligned} s_{k_0^d,t} &= \sqrt{G_b \beta l_{k_0^d,B_0}^{-\alpha}} \boldsymbol{u}_{k_0^d,t}^H \boldsymbol{H}_{k_0^d,B_0} \boldsymbol{V}_{k_0^d} \boldsymbol{s}_{k_0^d} \\ &+ \delta \sum_{j_0^u \in \phi_0'} \sqrt{\beta_u l_{k_0^d,j_0^u}^{-\alpha_u}} \boldsymbol{u}_{k_0^d}^H \boldsymbol{H}_{k_0^d,j_0^u} \boldsymbol{V}_{j_0^u} \boldsymbol{s}_{j_0^u} \\ &+ \sum_{B_q \in \Phi_M q \neq 0} \left(\sum_{i_q^d \in \tilde{\varphi}_q} \sqrt{G_b \beta l_{k_0^d,B_q}^{-\alpha}} \boldsymbol{u}_{k_0^d,t}^H \boldsymbol{H}_{k_0^d,B_q} \boldsymbol{V}_{i_q^d} \boldsymbol{s}_{i_q^d} \right. \\ &\left. + \sum_{j_q^u \in \phi_q} \sqrt{\beta_u l_{k_0^d,j_q^u}^{-\alpha}} \boldsymbol{u}_{k_0^d,t}^H \boldsymbol{H}_{k_0^d,j_q^u} \boldsymbol{V}_{j_q^u} \boldsymbol{s}_{j_q^u} \right) + \boldsymbol{u}_{k_0^d,t}^H \boldsymbol{n}_{k_0^d} \end{aligned} \tag{10}$$

where $\boldsymbol{u}_{k_0^d,t}$ is the tth column of $\boldsymbol{U}_{k_0^d}$. The SINR of the tth data stream at user k_0^d is given by

$$SINR_{k_0^d,t} = \frac{G_b \beta l_{k_0^d,B_0}^{-\alpha} P_d \parallel \boldsymbol{u}_{k_0^d,t}^H \boldsymbol{H}_{k_0^d,B_0} \boldsymbol{V}_{k_0^d} \parallel^2}{I_{inter}^d + I_{RUL}^d + \sigma^2}. \tag{11}$$

Here, $I_{inter}^d = I_{BS}^d + I_{UL}^d$ is the inter-cell interference power, while I_{BS}^d and I_{UL}^d denote the interference power from inter-cell BSs and UL users respectively. Thus, we have

$$I_{BS}^d = \sum_{B_q \in \Phi_M q \neq 0} G_b \beta l_{k_0^d,B_q}^{-\alpha} P_d \sum_{i_q^d \in \tilde{\varphi}_q} \parallel \boldsymbol{u}_{k_0^d,t}^H \boldsymbol{H}_{k_0^d,B_q} \boldsymbol{V}_{i_q^d} \parallel^2 \tag{12}$$

$$I_{UL}^d = \sum_{B_q \in \Phi_M q \neq 0} \beta_u P_u \sum_{j_q^u \in \phi_q} l_{k_0^d,j_q^u}^{-\alpha_u} \parallel \boldsymbol{u}_{k_0^d,t}^H \boldsymbol{H}_{k_0^d,j_q^u} \boldsymbol{V}_{j_q^u} \parallel^2 \tag{13}$$

and the power of residual intra-cell interference from UL users is given by

$$I_{RUL}^d = \delta \beta_u P_u \sum_{j_0^u \in \phi_0'} l_{k_0^d,j_0^u}^{-\alpha} \parallel \boldsymbol{u}_{k_0^d,t}^H \boldsymbol{H}_{k_0^d,j_0^u} \boldsymbol{V}_{j_0^u} \parallel^2 . \tag{14}$$

Applying the IA conditions, we have $\parallel \boldsymbol{u}_{k_0^d,t}^H \boldsymbol{H}_{k_0^d,B_0} \boldsymbol{V}_{k_0^d} \parallel^2 = \parallel \boldsymbol{u}_{k_0^d,t}^H \boldsymbol{H}_{k_0^d,B_0} \boldsymbol{v}_{k_0^d,t} \parallel^2$. Since all elements of channel matrices are i.i.d. complex normal random variables with zero mean and variance one, $\parallel \boldsymbol{u}_{k_0^d,t}^H \boldsymbol{H}_{k_0^d,B_0} \boldsymbol{V}_{k_0^d} \parallel^2$ is Chi-squared distributed with 2 degrees of freedom (DoF) (i.e. exponentially distributed with unit mean) and the conditional outage probability (also referred to as cumulative density function (CDF) of $SINR_{k_0^d,t}$) of the tth data stream at user k_0^d is given by

$$\begin{aligned} &\mathcal{P}\left(SINR_{k_0^d,t} < z | l_{k_0^d,B_0}\right) \\ &= 1 - \mathbb{E}\left[\exp\left(-\frac{z l_{k_0^d,B_0}^{\alpha}}{G_b \beta P_d}(I_{inter}^d + I_{RUL}^d + \sigma^2)\right)\right]. \end{aligned} \tag{15}$$

Using the fact that I_{inter}^d and I_{RUL}^d are independent, we have

$$\begin{aligned} &\mathcal{P}\left(SINR_{k_0^d,t} < z | l_{k_0^d,B_0}\right) \\ &= 1 - \mathcal{L}_{I_{inter}^d | l_{k_0^d,B_0}}(\mathcal{S}_d)\, \mathcal{L}_{I_{RUL}^d | l_{k_0^d,B_0}}(\mathcal{S}_d)\, e^{-\mathcal{S}_d \sigma^2} \end{aligned} \tag{16}$$

where $\mathcal{S}_d = \frac{z l_{k_0^d,B_0}^{\alpha}}{G_b \beta P_d}$, $\mathcal{L}_{I_{inter}^d | l_{k_0^d,B_0}}(\mathcal{S}_d) = \mathbb{E}_{I_{inter}^d}\left[e^{-\mathcal{S}_d I_{inter}^d}\right]$ and $\mathcal{L}_{I_{RUL}^d | l_{k_0^d,B_0}}(\mathcal{S}_d) = \mathbb{E}_{I_{RUL}^d}\left[e^{-\mathcal{S}_d I_{RUL}^d}\right]$ are the Laplace transform of I_{inter}^d and I_{RUL}^d, respectively, conditioned on given $l_{k_0^d,B_0}$.

Using the density function in (3), the unconditioned outage probability of k_0^d is obtained as

$$\mathcal{P}\left(SINR_{k_0^d,t} < z\right) = \int_0^R f_{l_{k_0^d,B_0}}(r) \mathcal{P}\left(SINR_{k_0^d,t} < z | r\right) dr. \tag{17}$$

Considering the inter-cell interference first, the expression for $\mathcal{L}_{I_{inter}^d | l_{k_0^d,B_0}}(\mathcal{S}_d)$ can be found in the following proposition.

Proposition 1. *For a given $l_{k_0^d,B_0}$, the coverage probability of the tth data stream at DL user k_0^d affected by inter-cell interference is given by (18), where $G_\varphi^d(x)$ can be written as*

$$G_\varphi^d(x) = (1-\delta)e^{-\mu_d(1-x)} + \delta\left(x^{K_d^{max}} + \sum_{K_d=0}^{K_d^{max}-1} P_d(K_d)\left(x^{K_d} - x^{K_d^{max}}\right)\right). \tag{19}$$

and $\mu_d = \pi R^2 \lambda_P^d$, $P_d(K_d) = e^{-\mu_d}\frac{(\mu_d)^{K_d}}{K_d!}$ is the probability that there are K_d DL users associated with the BS. $G_\phi^d(l,\theta)$ can be expressed as (20), $l_{B_0,j_q^u} = \sqrt{l^2+r^2-2lr\cos(\vartheta)}$, $\theta_{j_q^u} = \theta - \arcsin\left(\frac{r}{l_{B_0,j_q^u}}\sin(\vartheta)\right)$ and $\lambda_{MP} = -\frac{1}{\pi d_c^2}\ln(1-\pi d_c^2\lambda_M)$ [21] is the density of parent PPP. $\rho_M(l)$ is the conditional thinning probability of the MHCPP Φ_M given as

$$\rho_M(l) = \begin{cases} \rho_1(l) = \dfrac{\kappa_1(l,d_c)}{\kappa_2} & \text{if } d_c < l < 2d_c \\ \rho_2(l) = \dfrac{\lambda_M}{\lambda_{MP}} & \text{if } l \geq 2d_c \\ 0 & \text{otherwise.} \end{cases}. \tag{21}$$

Here, $\kappa_2 = \frac{1-\exp(-\lambda_{MP}\pi d_c^2)}{\lambda_{MP}\pi d_c^2}$ is the MHCPP retention probability [40] and $\kappa(l,d_c)$ can be written as [41]

$$\kappa_1(l,d_c) = \frac{1}{\lambda_{MP}^2}\left[\frac{1-e^{-S_0\lambda_{MP}}}{S_0^2 - S_0S_2(l,d_c)} + \frac{e^{\lambda_{MP}(S_2(l,d_c)-2S_0)}-1}{-3S_0S_2(l,d_c)+S_2(l,d_c)^2+2S_0^2} + \frac{\frac{1-e^{-\lambda_{MP}(S_1(l,d_c)-S_2(l,d_c)+S_0)}}{S_1(l,d_c)-S_2(l,d_c)+S_0} + \frac{e^{\lambda_{MP}(S_2(l,d_c)-2S_0)}-1}{2S_0-S_2(l,d_c)}}{S_0-S_1(l,d_c)}\right] \tag{22}$$

where $S_0 = \pi d_c^2$, $S_1(l,d_c)$ and $S_2(l,d_c)$ are given by

$$S_1(l,d_c) = \begin{cases} 2d_c^2\cos^{-1}\left(\dfrac{l}{2d_c}\right) - \dfrac{1}{2}l\sqrt{4d_c^2-l^2} & : 0 < l \leq 2d_c \\ 0 & : l > 2d_c \end{cases} \tag{23}$$

$$S_2(l,d_c) = \begin{cases} \pi l^2 & : 0 < l \leq d_c/2 \\ l^2\cos^{-1}\left(1-\dfrac{d_c^2}{2l^2}\right) + d_c^2\cos^{-1}\left(\dfrac{d_c}{2l}\right) - \dfrac{1}{2}d_c\sqrt{4l^2-d_c^2} & : l > \dfrac{d_c}{2} \end{cases}. \tag{24}$$

Proof. See Appendix A. □

Given the expression of $\mathcal{L}_{I_{inter}^d|l_{k_0^d,B_0}}(\mathcal{S}_d)$, $\mathcal{L}_{I_{UL}^d|l_{k_0^d,B_0}}(\mathcal{S}_d)$ (the coverage probability of the tth data stream at k_0^d affected by I_{UL}^d) can be obtained easily by setting $G_\varphi^d\left(\left(1+\frac{zl_{k_0^d,B_0}^\alpha}{(l_{k_0^d,B_0}^2+l^2-2l_{k_0^d,B_0}l\cos(\theta))^{\frac{\alpha}{2}}}\right)^{-b_d}\right) = 1$, i.e. $I_{BS}^d = 0$. Similarly, the coverage probability of the tth data stream at k_0^d affected by I_{BS}^d and denoted as $\mathcal{L}_{I_{BS}^d|l_{k_0^d,B_0}}(\mathcal{S}_d)$, can be obtained by substituting $G_\phi^d(l,\theta) = 1$ into (18). Moreover, when $d_c \gg R$ and $\delta = 1$, we provide a closed-form approximation of $\mathcal{L}_{I_{BS}^d|l_{k_0^d,B_0}}(\mathcal{S}_d)$ in following corollary.

Corollary 1. *For some given $l_{k_0^d,B_0}$, when $d_c \gg R$, $\delta = 1$ and the intensity of DL users is large enough, $\mathcal{L}_{I_{BS}^d|l_{k_0^d,B_0}}(\mathcal{S}_d)$ can be approximated as*

$$\hat{\mathcal{L}}_{I_{BS}^d|l_{k_0^d,B_0}}(\mathcal{S}_d) = F(K_d^{max}b_d, \lambda_M, A_{bu}, d_c, \alpha) \tag{25}$$

where $A_{bu} = \mathcal{S}_d G_b \beta P_d = z l_{k_0^d,B_0}^\alpha$, function $F(b,\lambda,A,x,\alpha)$ is given by

$$F(b,\lambda,A,x,\alpha) = \exp\left[-\sum_{p=0}^{b-1}\binom{p}{b}\frac{2\pi\lambda x^2}{\alpha(b-p)-2}\left(\frac{A}{x^\alpha}\right)^{b-p} \times 2F1\left(b, b-(p+\frac{2}{\alpha}); b-(p+\frac{2}{\alpha})+1; -\frac{A}{x^\alpha}\right)\right] \tag{26}$$

and $2F1(a,b;c;d)$ is hypergeometric function [42, 9.14.1].

Proof. See Appendix B. □

For the possible intra-cell interference, the coverage probability of the tth data stream at DL user k_0^d affected by intra-cell UL users is given in Proposition 2.

Proposition 2. *For some given $l_{k_0^d,B_0}$, the coverage probability of the tth data stream at DL user k_0^d affected by intra-cell UL users can be written as (27), where $P(K_u) = \exp(-\lambda_P^u\pi R^2)\frac{(\lambda_P^u\pi R^2)^{K_u}}{K_u!}$ is the probability that there are K_u UL users in the cell of B_0, $A_{uu} = \mathcal{S}_d\beta_u P_u$, $l_{k_0^d,j_0^u} = (l_{k_0^d,B_0}^2 + l_{B_0,j_0^u}^2 - 2l_{k_0^d,B_0}l_{B_0,j_0^u}\cos\theta)^{1/2}$, and $f_{K_u^{max}}(r)$ is the PDF of distance from B_0 to the K_u^{max}th nearest UL user and is given by [43]*

$$f_{K_u^{max}}(r) = e^{-\lambda_P^u\pi r^2}\frac{2\left(\lambda_P^u\pi r^2\right)^{K_u^{max}}}{r\Gamma(K_u^{max})} \tag{28}$$

where $\Gamma(\cdot)$ is Gamma function.

Proof. See Appendix C. □

Up to this point, we have obtained expressions for $\mathcal{L}_{I_{inter}^d|l_{k_0^d,B_0}}(\mathcal{S}_d)$ and $\mathcal{L}_{I_{RUL}^d|l_{k_0^d,B_0}}(\mathcal{S}_d)$. The outage probability of the tth data stream of user k_0^d can be obtained by substituting for $\mathcal{L}_{I_{inter}^d|l_{k_0^d,B_0}}(\mathcal{S}_d)$ and $\mathcal{L}_{I_{RUL}^d|l_{k_0^d,B_0}}(\mathcal{S}_d)$ into (16).

When $P_d \gg P_u$, interference from inter-cell BSs becomes dominant and $\mathcal{P}\left(SINR_{k_0^d,t} < z|l_{k_0^d,B_0}\right)$ can be approximated as $1 - \mathcal{L}_{I_{inter}^d|l_{k_0^d,B_0}}(\mathcal{S}_d)e^{-\mathcal{S}_d\sigma^2}$. Moreover, assuming $d_c \gg R$, we have $\mathcal{L}_{I_{inter}^d|l_{k_0^d,B_0}}(\mathcal{S}_d) \approx \hat{\mathcal{L}}_{I_{BS}^d|l_{k_0^d,B_0}}(\mathcal{S}_d)$, which has been given in (25). Therefore, when $P_d \gg P_u$

$$\mathcal{L}_{I^d_{inter}|l_{k_0^d,B_0}}(\mathcal{S}_d)=\exp\left\{-\int_0^{2\pi}\int_{d_c}^{\infty}\left(1-G_\varphi^d\left(\left(1+\frac{\mathcal{S}_d G_b\beta P_d}{(l^2_{k_0^d,B_0}+l^2-2l_{k_0^d,B_0}l\cos(\theta))^{\frac{\alpha}{2}}}\right)^{-b_d}\right)G_\phi^d(l,\theta)\right)\lambda_{MP}\rho_M(l)l dl d\theta\right\} \tag{18}$$

$$G_\phi^d(l,\theta)=\exp\left[-\lambda_P^u\int_0^{2\pi}\int_0^{R}\left(1-\left(1+\frac{\mathcal{S}_d\beta_u P_u}{\left(l^2_{B_0,j_q^u}+l^2_{k_0^d,B_0}-2l_{B_0,j_q^u}l_{k_0^d,B_0}\cos\left(\theta_{j_q^u}\right)\right)^{\alpha_u/2}}\right)^{-b_u}\right)r dr d\vartheta\right] \tag{20}$$

$$\mathcal{L}_{I^d_{RUL}|l_{k_0^d,B_0}}(\mathcal{S}_d)=1-\delta+\delta\left\{\sum_{K_u=0}^{K_u^{max}-1}P(K_u)+\int_{r=0}^{R}f_{K_u^{max}}(r)\exp\left[-\lambda_P^u\int_0^{2\pi}\int_r^R\left(1-\left(1+\frac{A_{uu}}{l^\alpha_{k_0^d,j_0^u}}\right)^{-b_u}\right)l dl d\theta\right]dr\right\} \tag{27}$$

and $d_c \gg R$, we have

$$\mathcal{P}\left(SINR_{k_0^d,t}<z|l_{k_0^d,B_0}\right)\approx 1-F(K_d^{max}b_d,\lambda_M,A_{bu},d_c,\alpha)\exp\left(-\mathcal{S}_d\sigma^2\right). \tag{29}$$

2) Throughput of DL user k_0^d

Since each DL user receives b_d data streams from the corresponding BS, the throughput of DL user k_0^d can be expressed as

$$\begin{aligned}T_{k_0^d}&=b_d\mathcal{R}\left(1-\mathcal{P}\left(SINR_{k_0^d,t}<z|l_{k_0^d,B_0}\right)\right)\\&=b_d\mathcal{R}\mathcal{L}_{I^d_{inter}|l_{k_0^d,B_0}}(\mathcal{S}_d)\mathcal{L}_{I^d_{RUL}|l_{k_0^d,B_0}}(\mathcal{S}_d)\exp\left(-\mathcal{S}_d\sigma^2\right)\end{aligned} \tag{30}$$

where $\mathcal{R}$ is the required data rate and $z=2^{\mathcal{R}}-1$.

Assuming $d_c \gg R$ and in the high P_d/P_u regime, the throughput of DL user k_0^d can be approximated as

$$T_{k_0^d}\approx b_d\mathcal{R}F(K_d^{max}b_d,\lambda_M,A_{bu},d_c,\alpha)\exp\left(-\mathcal{S}_d\sigma^2\right). \tag{31}$$

3) Capacity of the channel between BS and a generic DL user

For DL user k_0^d, the link capacity can be written as

$$\begin{aligned}C_{k_0^d|l_{k_0^d,B_0}}&=\mathbb{E}\left[b_d\log_2\left(1+SINR_{k_0^d,t}\right)\right]\\&=\mathbb{E}\left[b_d\log_2\left(1+\frac{l^{-\alpha}_{k_0^d,B_0}G_b\beta P_d\parallel \boldsymbol{u}^H_{k_0^d,t}\boldsymbol{H}_{k_0^d,B_0}\boldsymbol{V}_{k_0^d}\parallel^2}{I^d_{inter}+I^d_{RUL}+\sigma^2}\right)\right].\end{aligned} \tag{32}$$

Invoking (9), $C_{k_0^d|l_{k_0^d,B_0}}$ can be rewritten as

$$\begin{aligned}C_{k_0^d|l_{k_0^d,B_0}}&=\frac{b_d}{\ln 2}\int_0^\infty\mathbb{E}\left[e^{-\frac{z}{\sigma^2}\left(I^d_{inter}+I^d_{RUL}\right)}\right]\\&\times\left(1-\mathbb{E}\left[e^{-\frac{zG_b\beta P_d}{\sigma^2 l^\alpha_{k_0^d,B_0}}\parallel\boldsymbol{u}^H_{k_0^d,t}\boldsymbol{H}_{k_0^d,B_0}\boldsymbol{V}_{k_0^d}\parallel^2}\right]\right)\frac{e^{-z}}{z}dz\\&=\frac{b_d}{\ln 2}\int_0^\infty\mathcal{L}_{I^d_{inter}|l_{k_0^d,B_0}}\left(\frac{z}{\sigma^2}\right)\mathcal{L}_{I^d_{RUL}|l_{k_0^d,B_0}}\left(\frac{z}{\sigma^2}\right)\\&\times\frac{e^{-z}G_b\beta P_d}{\sigma^2 l^\alpha_{k_0^d,B_0}+zG_b\beta P_d}dz\end{aligned} \tag{33}$$

where the expressions for $\mathcal{L}_{I^d_{inter}|l_{k_0^d,B_0}}(\mathcal{S}_d)$ and $\mathcal{L}_{I^d_{RUL}|l_{k_0^d,B_0}}(\mathcal{S}_d)$ are already known from (18) and (27).

In particular, when $d_c \gg R$, $\delta=1$ and in the high P_d/P_u regime, the link capacity can be approximated as

$$\begin{aligned}\hat{C}_{k_0^d|l_{k_0^d,B_0}}&=\frac{b_d}{\ln 2}\int_0^\infty F\left(K_d^{max}b_d,\lambda_M,\frac{zG_b\beta P_d}{\sigma^2},d_c,\alpha\right)\\&\times\frac{e^{-z}G_b\beta P_d}{\sigma^2 l^\alpha_{k_0^d,B_0}+zG_b\beta P_d}dz.\end{aligned} \tag{34}$$

For a generic DL user, (33) can be unconditioned to obtain

$$C_{k_0^d}=\int_{l_{k_0^d,B_0}=0}^{R}f(l_{k_0^d})C_{k_0^d|l_{k_0^d,B_0}}dl_{k_0^d,B_0}. \tag{35}$$

B. PERFORMANCE OF A GENERIC UL USER SERVED BY FD BS

1) Outage probability for each data stream of a generic UL user

Consider UL transmission, it is assumed that all BSs perform single-stream decoding. The tth data stream from UL user k_0^u can be written as (36), where $\boldsymbol{u}_{k_0^u,t}$ is the tth column of $\boldsymbol{U}_{k_0^u}$. The SINR of the tth data stream from UL user K_0^u can be expressed as

$$SINR_{k_0^u,t}=\frac{l^{-\alpha}_{B_0,k_0^u}G_b\beta P_u\parallel\boldsymbol{u}^H_{k_0^u,t}\boldsymbol{H}_{B_0,k_0^u}\boldsymbol{V}_{k_0^u}\parallel^2}{I_{SI}+I^u_{RUL}+I^u_{inter}+\sigma^2} \tag{37}$$

where $I_{SI}=\sum_{i_0^d\in\tilde{\varphi}_0}G_b^2\beta_b P_d\parallel\boldsymbol{u}^H_{k_0^u,t}\hat{\boldsymbol{H}}_{B_0,B_0}\boldsymbol{V}_{i_0^d}\parallel^2$ is the power of the residual SI, and I^u_{RUL} and $I^u_{inter}=I^u_{BS}+I^u_{UL}$ are the power of intra-cell and inter-cell interference. Here, I^u_{RUL}, I^u_{BS} and I^u_{UL} are respectively given by

$$I^u_{RUL}=\delta\sum_{j_0^u\in\phi_0'}l^{-\alpha}_{B_0,j_0^u}G_b\beta P_u\parallel\boldsymbol{u}^H_{k_0^u,t}\boldsymbol{H}_{B_0,j_0^u}\boldsymbol{V}_{j_0^u}\parallel^2 \tag{38}$$

$$I^u_{BS}=\sum_{B_q\in\Phi_M q\neq 0}\sum_{i_q^d\in\tilde{\varphi}_q}l^{-\alpha_b}_{B_0,B_q}G_b^2\beta_b P_d\parallel\boldsymbol{u}^H_{k_0^u,t}\boldsymbol{H}_{B_0,B_q}\boldsymbol{V}_{i_q^d}\parallel^2 \tag{39}$$

$$I^u_{UL}=\sum_{B_q\in\Phi_M q\neq 0}\sum_{j_q^u\in\phi_q}l^{-\alpha}_{B_0,j_q^u}G_b\beta P_u\parallel\boldsymbol{u}^H_{k_0^u,t}\boldsymbol{H}_{B_0,j_q^u}\boldsymbol{V}_{j_q^u}\parallel^2. \tag{40}$$

$$s_{k_0^u,t} = \sqrt{G_b\beta l_{B_0,k_0^u}^{-\alpha}}\boldsymbol{u}_{k_0^u,t}^H \boldsymbol{H}_{B_0,k_0^u}\boldsymbol{V}_{k_0^u}\boldsymbol{s}_{k_0^u} + \sum_{i_0^d\in\tilde{\varphi}_0}\sqrt{G_b^2\beta_b}\boldsymbol{u}_{k_0^u,t}^H\hat{\boldsymbol{H}}_{B_0,B_0}\boldsymbol{V}_{i_0^d}\boldsymbol{s}_{i_0^d} + \delta\sum_{j_0^u\in\phi_0'}\sqrt{\frac{G_b\beta}{l_{B_0,j_0^u}^{-\alpha}}}\boldsymbol{u}_{k_0^u}^H\boldsymbol{H}_{B_0,j_0^u}\boldsymbol{V}_{j_0^u}\boldsymbol{s}_{j_0^u}$$
$$+\sum_{B_q\in\Phi_M q\neq 0}\left(\sum_{i_q^d\in\tilde{\varphi}_q}\sqrt{G_b^2\beta_b l_{B_0,B_q}^{-\alpha_b}}\boldsymbol{u}_{k_0^u,t}^H\boldsymbol{H}_{B_0,B_q}\boldsymbol{V}_{i_q^d}\boldsymbol{s}_{i_q^d} + \sum_{j_q^u\in\phi_q}\sqrt{G_b\beta l_{B_0,j_q^u}^{-\alpha}}\boldsymbol{u}_{k_0^u,t}^H\boldsymbol{H}_{B_0,j_q^u}\boldsymbol{V}_{j_q^u}\boldsymbol{s}_{j_q^u}\right) + \boldsymbol{u}_{k_0^u,t}^H\boldsymbol{n}_{k_0^d} \quad (36)$$

Therefore, given the distance between UL user k_0^u and BS B_0, the conditional outage probability of the tth data stream from UL user k_0^u can be written as

$$\mathcal{P}\left(SINR_{k_0^u,t} < z|l_{B_0,k_0^u}\right) = 1 - \mathcal{L}_{I_{SI}|l_{B_0,k_0^u}}(\mathcal{S}_u)$$
$$\times\,\mathcal{L}_{I_{RUL}^u|l_{B_0,k_0^u}}(\mathcal{S}_u)\mathcal{L}_{I_{inter}^u|l_{B_0,k_0^u}}(\mathcal{S}_u)\exp\left(-\mathcal{S}_u\sigma^2\right) \quad (41)$$

where $\mathcal{S}_u = \frac{zl_{B_0,k_0^u}^{\alpha}}{G_b\beta P_u}$, $\mathcal{L}_{I_{SI}|l_{B_0,k_0^u}}(\mathcal{S}_u) = \mathbb{E}_{I_{SI}}\left[e^{-\mathcal{S}_u I_{SI}}\right]$, $\mathcal{L}_{I_{RUL}^u|l_{B_0,k_0^u}}(\mathcal{S}_u) = \mathbb{E}_{I_{RUL}^u}\left[e^{-\mathcal{S}_u I_{RUL}^u}\right]$ and $\mathcal{L}_{I_{inter}^u|l_{B_0,k_0^u}}(\mathcal{S}_u) = \mathbb{E}_{I_{inter}^u}\left[e^{-\mathcal{S}_u I_{inter}^u}\right]$.

Given the PDF of l_{B_0,k_0^u} in (3), the unconditional outage probability of UL user k_0^u can be computed as

$$\mathcal{P}\left(SINR_{k_0^u,t} < z\right) = \int_0^R f_{l_{B_0,k_0^u}}(r)\mathcal{P}\left(SINR_{k_0^u,t} < z|r\right)dr. \quad (42)$$

Considering the residual SI first, the coverage probability is given in following proposition.

Proposition 3. *For given l_{B_0,k_0^u}, the coverage probability of the tth data stream from UL user k_0^u affected by the residual SI at BS is given by*

$$\mathcal{L}_{I_{SI}|l_{B_0,k_0^u}}(\mathcal{S}_u) = G_\varphi^d\left(\left(1+\mathcal{S}_u G_b^2\beta_{b_1}P_d\sigma_s^2\right)^{-b_d}\right), \quad (43)$$

where $G_\varphi^d(x)$ has been provided in (19).

Proof. See Appendix D. □

With respect to inter-cell interference, the coverage probability of the tth data stream from UL user k_0^u is given in Proposition 4.

Proposition 4. *Given the distance between UL user k_0^u and BS B_0, the coverage probability of the tth data stream from UL user k_0^u affected by the inter-cell interference can be written as*

$$\mathcal{L}_{I_{inter}^u|l_{B_0,k_0^u}}(\mathcal{S}_u)$$
$$= \exp\left[-2\pi\int_{d_c}^{\infty}\left(1 - G_\varphi^d\left(\left(1+\frac{A_{ub}}{l_{B_0,B_q}^{\alpha_b}}\right)^{-b_d}\right)\right.\right.$$
$$\left.\left.\times G_\phi^u(l_{B_0,B_q})\right)\lambda_{MP}\rho_M(l_{B_0,B_q})l_{B_0,B_q}dl_{B_0,B_q}\right] \quad (44)$$

where $A_{ub} = \mathcal{S}_u G_b^2\beta_b P_d$ and $G_\phi^u(l_{B_0,B_q})$ is given by

$$G_\phi^u(l_{B_0,B_q}) = \exp\left[-\lambda_P^u\int_0^{2\pi}\int_0^R\left(1-\left(1\right.\right.\right.$$
$$\left.\left.\left.+\frac{\mathcal{S}_u G_b\beta P_u}{\left(l_{B_0,B_q}^2 + r^2 - 2l_{B_0,B_q}r\cos(\vartheta)\right)^{\alpha/2}}\right)^{-b_u}\right)rdrd\vartheta\right]. \quad (45)$$

Proof. The proof of Proposition 4 follows steps similar to those outlined in the proof of Proposition 1, and is thus omitted. □

For the tth data stream from k_0^u, the expressions of coverage probabilities affected by I_{BS}^u and I_{UL}^u can be obtained by substituting $G_\phi^u(l_{B_0,B_q}) = 1$ and $G_\varphi^d\left(\left(1+\frac{A_{ub}}{l_{B_0,B_q}^{\alpha_b}}\right)^{-b_d}\right) = 1$ into (44) respectively.

Corollary 2. *Given the distance between UL user k_0^u and B_0, the coverage probability of the tth data stream from UL user k_0^u affected by inter-cell interference from DL BSs can be approximated as*

$$\hat{\mathcal{L}}_{I_{BS}^u}(\mathcal{S}_u) = \frac{F(K_d^{max}b_d,\lambda_M,A_{ub},d_c,\alpha_{b_1})}{F(K_d^{max}b_d,\lambda_M,A_{ub},R_c,\alpha_{b_1})}$$
$$\times\,F(K_d^{max}b_d,\lambda_M,A_{ub},R_c,\alpha_{b_2}). \quad (46)$$

Proof. The proof of Corollary 2 follows steps similar to those outlined in the proof of Corollary 1, and is thus omitted. □

As for the interference from intra-cell UL users, the coverage probability can be found in following proposition.

Proposition 5. *For some given l_{B_0,k_0^u}, the coverage probability of the tth data stream from UL user k_0^u affected by the residual intra-cell interference from UL users is given by (47).*

Proof. The proof of Proposition 5 follows steps similar to those outlined in the proof of Proposition 2, and is thus omitted. □

To this point, the expressions for $\mathcal{L}_{I_{SI}|l_{B_0,k_0^u}}(\mathcal{S}_u)$, $\mathcal{L}_{I_{BS}^u|l_{B_0,k_0^u}}(\mathcal{S}_u)$, $\mathcal{L}_{I_{RUL}^u|l_{B_0,k_0^u}}(\mathcal{S}_u)$ and $\mathcal{L}_{I_{UL}^u|l_{B_0,k_0^u}}(\mathcal{S}_u)$ have been derived, the conditional outage probability of the tth data stream from UL user k_0^u can be obtained by substituting these into (41).

Since users are randomly distributed in the circular region centered around their corresponding BS, the locations of the user are dependent on the locations of the BSs. However, it is reasonable to assume that the user locations are independent with the BS location when analysing the inter-cell interference. This assumption has been proved to be tight in [18]. Therefore, when $P_d \gg P_u$, $\mathcal{P}(SINR_{k_0^u} < z|l_{B_0,k_0^u})$ can be approximated as

$$\hat{\mathcal{P}}(SINR_{k_0^u} < z|l_{B_0,k_0^u}) = 1 - \mathcal{L}_{I_{SI}|l_{B_0,k_0^u}}(\mathcal{S}_u)$$
$$\times\,\hat{\mathcal{L}}_{I_{BS}^u|l_{B_0,k_0^u}}(\mathcal{S}_u)\exp\left(-\mathcal{S}_u\sigma^2\right). \quad (48)$$

$$\mathcal{L}_{I^u_{RUL}|l_{B_0,k_0^u}}(\mathcal{S}_u) = 1-\delta+\delta\left\{\sum_{K_u=0}^{K_u^{max}-1} P(K_u) + \int_{l_{B_0,k_0^u}}^{R} f_{K_u^{max}}(r)\left(1+\frac{\mathcal{S}_u G_b \beta P_u}{r^\alpha}\right)^{-b_u} \frac{F(bu,\lambda_P^u,\mathcal{S}_u G_b\beta P_u, r)}{F(bu,\lambda_P^u,\mathcal{S}_u G_b\beta P_u, R)} dr\right\} \quad (47)$$

2) Throughput of UL user k_0^u

The throughput of link between UL user k_0^u and its associated BS can be expressed as

$$\begin{aligned} T_{k_0^u} &= b_u \mathcal{R}\left(1-\mathcal{P}\left(SINR_{k_0^u,t} < z | l_{B_0,k_0^u}\right)\right) \\ &= b_u \mathcal{R} \mathcal{L}_{I_{SI}|l_{B_0,k_0^u}}(\mathcal{S}_u) \mathcal{L}_{I^u_{inter}|l_{B_0,k_0^u}}(\mathcal{S}_u) \\ &\quad \times \mathcal{L}_{I^u_{RUL}|l_{B_0,k_0^u}}(\mathcal{S}_u) e^{-\mathcal{S}_u\sigma^2}. \end{aligned} \quad (49)$$

Assuming $P_d \gg P_u$, $T_{k_0^u}$ can be approximated as

$$\hat{T}_{k_0^u} = b_u \mathcal{R} \mathcal{L}_{I_{SI}|l_{B_0,k_0^u}}(\mathcal{S}_u) \hat{\mathcal{L}}_{I^u_{BS}|l_{B_0,k_0^u}}(\mathcal{S}_u) e^{-\mathcal{S}_u\sigma^2}. \quad (50)$$

3) Capacity of the link between a generic UL user and BS

For UL user k_0^u, the conditional link capacity is given by

$$\begin{aligned} C_{k_0^u|l_{B_0,k_0^u}} &= \mathbb{E}\left[b_u \log_2\left(1+SINR_{k_0^u,t}\right)\right] \\ &= \frac{b_u}{\ln 2}\int_0^\infty \mathcal{L}_{I_{SI}|l_{B_0,k_0^u}}\left(\frac{z}{\sigma^2}\right) \mathcal{L}_{I^u_{inter}|l_{B_0,k_0^u}}\left(\frac{z}{\sigma^2}\right) \\ &\quad \times \mathcal{L}_{I^u_{RUL}|l_{B_0,k_0^u}}\left(\frac{z}{\sigma^2}\right) \frac{e^{-z} G_b \beta P_u}{\sigma^2 l^\alpha_{B_0,k_0^u} + z G_b \beta P_u} dz. \end{aligned} \quad (51)$$

When $P_d \gg P_u$, the conditional link capacity can be approximated as

$$\begin{aligned} \hat{C}_{k_0^u|l_{B_0,k_0^u}} &= \frac{b_u}{\ln 2}\int_0^\infty \mathcal{L}_{I_{SI}|l_{B_0,k_0^u}}\left(\frac{z}{\sigma^2}\right) \hat{\mathcal{L}}_{I^u_{BS}|l_{B_0,k_0^u}}\left(\frac{z}{\sigma^2}\right) \\ &\quad \times \frac{e^{-z} G_b \beta P_u}{\sigma^2 l^\alpha_{B_0,k_0^u} + z G_b \beta P_u} dz. \end{aligned} \quad (52)$$

For a generic UL user, the unconditional link capacity can be expressed as

$$C_{k_0^u} = \int_0^R f_{l_{B_0,k_0^u}}(r) C_{k_0^u|r} dr. \quad (53)$$

C. PERFORMANCE OF HD SYSTEMS

To compare the performance of FD and HD networks, we provide expressions for the capacity in HD networks. Since separate time-frequency signaling channels are utilized for DL and UL transmissions in HD communication, we scale the capacity of a fully DL or UL HD network by $1/2$, so as to provide a fair comparison with FD.

By turning off the UL user transmission, we have $I^d_{UL}=0$ and $I^d_{RUL}=0$. Thus, the link capacity of DL user k_0^d (i.e. the counterpart to (33)) can be written as

$$C^{HD}_{k_0^d|l_{k_0^d,B_0}} = \frac{1}{2}\frac{b_d}{\ln 2}\int_0^\infty \mathcal{L}_{I^d_{BS}}\left(\frac{z}{\sigma^2}\right) \frac{e^{-z} G_b \beta P_d}{\sigma^2 l^\alpha_{k_0^d,B_0} + z G_b \beta P_d} dz. \quad (54)$$

Assuming $d_c \gg R$ and $\delta = 1$, we have

$$\begin{aligned} \hat{C}^{HD}_{k_0^d|l_{k_0^d,B_0}} &= \frac{1}{2}\frac{b_d}{\ln 2}\int_0^\infty F\left(K_d^{max} b_d, \lambda_M, \frac{z G_b \beta P_d}{\sigma^2}, d_c, \alpha\right) \\ &\quad \times \frac{e^{-z} G_b \beta P_d}{\sigma^2 l^\alpha_{k_0^d,B_0} + z G_b \beta P_d} dz. \end{aligned} \quad (55)$$

For UL user k_0^u, the HD counterpart to (51) can be obtained by turning off BS transmission (i.e. $I_{SI}=0$ and $I^u_{BS}=0$) and written as

$$\begin{aligned} C^{HD}_{k_0^u|l_{B_0,k_0^u}} &= \frac{1}{2}\frac{b_u}{\ln 2}\int_0^\infty \mathcal{L}_{I^u_{UL}|l_{B_0,k_0^u}}\left(\frac{z}{\sigma^2}\right) \\ &\quad \times \mathcal{L}_{I^u_{RUL}|l_{B_0,k_0^u}}\left(\frac{z}{\sigma^2}\right) \frac{e^{-z} G_b \beta P_u}{\sigma^2 l^\alpha_{B_0,k_0^u} + z G_b \beta P_u} dz. \end{aligned} \quad (56)$$

Assuming $\delta = 1$, we have

$$\hat{C}^{HD}_{k_0^u|l_{B_0,k_0^u}} = \frac{1}{2}\frac{b_u}{\ln 2}\int_0^\infty \mathcal{L}_{I^u_{UL}}\left(\frac{z}{\sigma^2}\right) \frac{e^{-z} G_b \beta P_u}{\sigma^2 l^\alpha_{B_0,k_0^u} + z G_b \beta P_u} dz. \quad (57)$$

V. NUMERICAL RESULTS

In this section, Monte Carlo simulations are used to verify the accuracy of the derived expressions. We also study the effect of varying the hard-core distance between the BSs, and applying IA to each cell. Two different network settings are considered, namely, (a) a micro-cell scenario, and (b) a macro-cell scenario. Throughout all the simulations, unless otherwise specified, we assume $M_u = M_d = 10$, $N_d = N_u = 6$, $b_d = b_u = 2$ and $l_{k_0^d,B_0} = l_{B_0,k_0^u} = 100m$. For micro-cellular networks, we assume $R = 300m$, $d_c = 290m$, $\lambda_M = 3.54\ BSs/km^2$ (i.e. one BS per circular cell of radius 300 m) and $\lambda^d_P = \lambda^u_P = 7.08\ users/km^2$. As for macro-cellular networks, it is assumed that $R = 1000m$, $d_c = 950m$, $\lambda_M = 0.32\ BSs/km^2$ (i.e. one BS per circular cell of radius 1000 m) and $\lambda^d_P = \lambda^u_P = 3.84\ users/km^2$. All the other parameters are provided in Table 1.

For a FD micro-cellular network, CDFs of DL and UL SINR are plotted versus targeted SINR in Fig. 3. It can be observed that both DL and UL transmissions are feasible in FD micro-cellular networks and DL transmission outperforms UL transmission. This is because different pathloss parameters are applied to BS-BS and BS-user links, and UL transmission suffers more significant interference from BSs with distances below R_c.

For randomly distributed DL and UL users in a FD micro-cellular network where $\lambda_{MP} = 3.54\ BSs/km^2$ and targeted SINR=-5 dB, outage probabilities are plotted versus hard-core distance in Fig. 4 where different numbers of data streams required at each user are considered. It can be noticed from Fig. 4, that outage probabilities decrease with hard-

TABLE 1: Parameters for different networks

Parameter	P_d	P_u	G_b	α	α_{b_1}	α_{b_2}	α_u
Micro-cell	24 dBm	23 dBm	5 dBi	3.75	3	4	4
Macro-cell	46 dBm	23 dBm	15 dBi	3.75	3	4	4
Parameter	β	β_{b_1}	β_{b_2}	β_u	h_{BS}	ξ	R_c
Micro-cell	-32.9 dB	-38.45 dB	-49.36 dB	-55.78 dB	4m	0.15m	427m
Macr-ocell	-15.3 dB	-38.45 dB	1.0439 dB	-55.78 dB	20m	0.15m	10667m

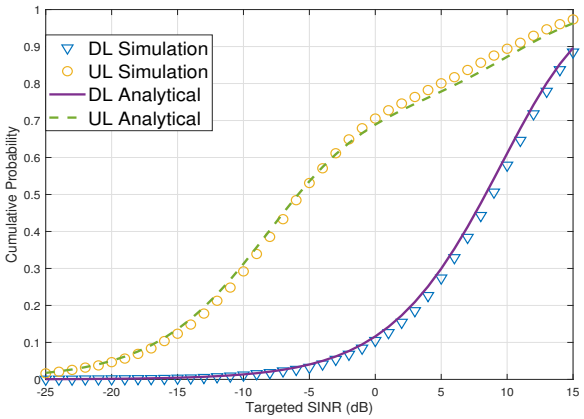

FIGURE 3: CDFs of DL and UL SINR in a full-duplex micro-cellular network.

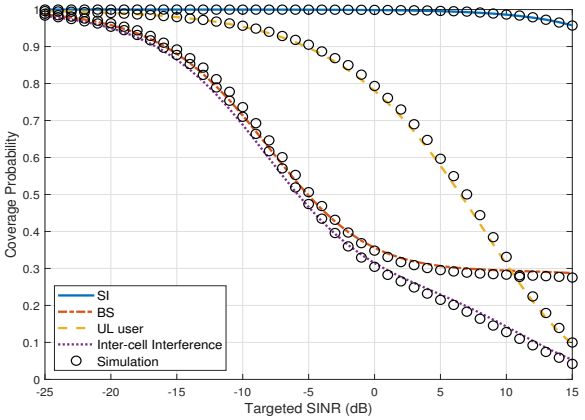

FIGURE 5: Coverage probability of UL user affected by different interferences in a full-duplex micro-cellular network.

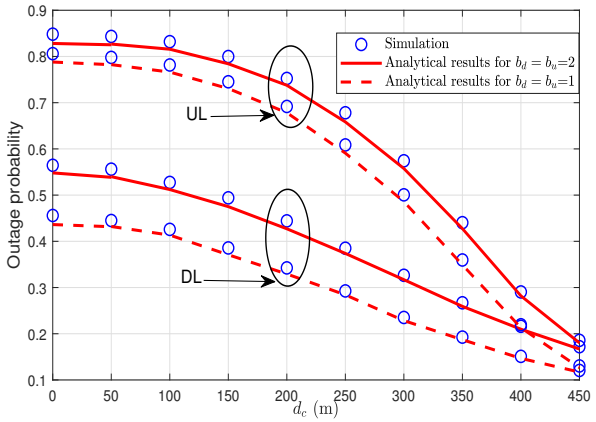

FIGURE 4: Outage probabilities of randomly distributed DL and UL users in a full-duplex micro-cellular network.

core distance. When hard-core distance is greater than critical distance R_c, UL and DL users experience almost the same outage probability. This is because BSs and users in micro-cellular networks have similar transmit power and BSs within critical distance suffer less path loss than these with distances to B_0 greater than critical distance. Moreover, Fig. 4 shows that outage probabilities of DL and UL users can be improved by reducing the number of data streams required at each user. When $d_c = 0$, HCPP converges to PPP and it can be observed that FD transmission in PPP-based model may be infeasible and a suitable distance between BSs should be imposed.

Consider a micro-cellular network, the effect of different interferences on UL transmission are studied in Fig. 5 where the coverage probabilities of a UL user with link length l_{B_0,k_0^u} are plotted against SINR. Assuming an analog/digital SI cancellation scheme is adopted at each BS, the covariance of elements in the residual SI channel is specified as $\sigma_s^2 = -110$ dB [6]. Due to the low BS-BS pathloss for distances below R_c, it can be noticed that inter-cell interference among BSs has much more significant impact on UL transmission than interference from UL users. Since we adopt a two-slope model for the BS-BS pathloss, interference from BSs with distance to the origin below R_c is dominant. Therefore, in the high SINR regime, the coverage probability of a UL user affected by inter-cell interference from BSs converges to a fixed value which is the probability that there is no interferer BS with distance to the origin less than R_c. The average number of BSs distributed within R_c can be calculated as $\mu = \int_{d_c}^{R_c} 2\pi r \lambda_M \rho_M(r) dr$. Then, we have $e^{-\mu} = 0.2435$ which matches the result in Fig. 5. Moreover, due to the use of SI cancellation scheme and low DL transmission power in micro-cell networks, SI plays an inconsequential role in UL transmission. It can be concluded that UL transmission in micro-cell networks is mainly affected by inter-cell interference from BSs and UL users when an SI cancellation scheme is applied at each BS.

Assuming BSs have limited number of transmit antenna, the CDFs of UL SINR at BSs in a FD micro-cell network are characterized as shown in Fig. 6. In Fig.6a, we set $K_d^{max} = 4$ and vary K_u^{max}, the maximum numbers of UL user which allow IA to still be feasible. Fig. 6a shows that UL performance can be improved by increasing K_u^{max}, i.e. increasing the number of antenna at each BS. Since UL users

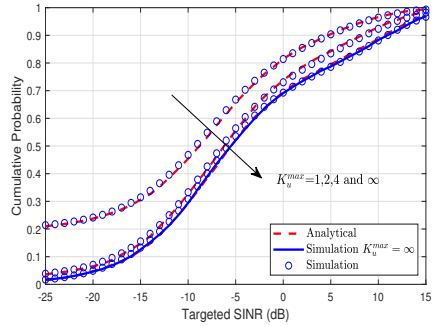

(a) K_u^{max} comparison

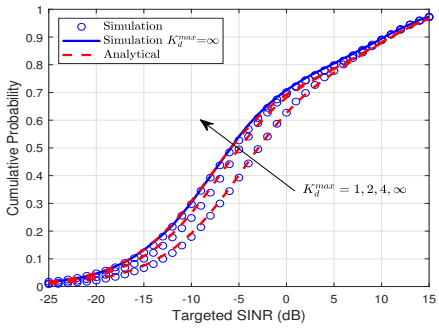

(b) K_d^{max} comparison

FIGURE 6: CDFs of SINR at a UL user in a FD micro-cellular network with limited number of transmit antennas at BS.

are distributed as a PPP, when $K_u > K_u^{max}$, only the nearest K_u^{max} UL users are served while the rest $K_u - K_u^{max}$ users are treated as interferers. Therefore, increasing K_u^{max} will suppress the intra-cell interference. Different from Fig.6a, in Fig.6b we set $K_u^{max} = 4$ and vary K_d^{max}. It can be observed that increasing K_d^{max} has a negative impact on UL performance, since the inter-cell interference from BSs increases with K_d^{max}. However, it worth to be noticed that in low and high targeted SINR regimes, the UL performance could not be improved by reducing K_d^{max}. By increasing K_u^{max} or K_d^{max}, it can be recognized that the performance gap between $K_u^{max} \geq 2\pi R^2 \lambda_P^u$ (or $K_d^{max} \geq 2\pi R^2 \lambda_P^d$) (i.e. Case II and in this case $K_u^{max} = 4$ (or $K_d^{max} = 4$)) and $K_u^{max} = \infty$ (or $K_d^{max} = \infty$) (i.e. Case I) is uniformly marginal. Therefore, by setting $K_u^{max} \geq 2\pi R^2 \lambda_P^u$ or $K_d^{max} \geq 2\pi R^2 \lambda_P^d$, Case II converges to Case I and the intra-cell interference is marginal and can be ignored. In the remainder of this paper, we assume $K_u^{max} = K_d^{max} = \infty$.

For a macro-cellular network, the throughput of DL and UL users are plotted against hard-core distance in Fig. 7 when the targeted data rate $r_t = 2$ bits per channel use. It can be observed that our approximations match simulation results quite closely. In the small hard-core distance regime, it can be seen that UL transmission provides poor performance, while DL has much better performance than UL. This is caused by the fact that DL transmission power from BSs is much larger than UL transmission power from users, and SI at BSs

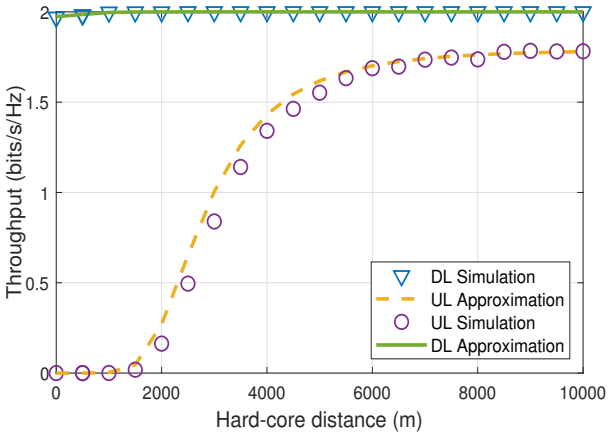

FIGURE 7: Throughput of DL and UL users in a full-duplex macro-cellular network.

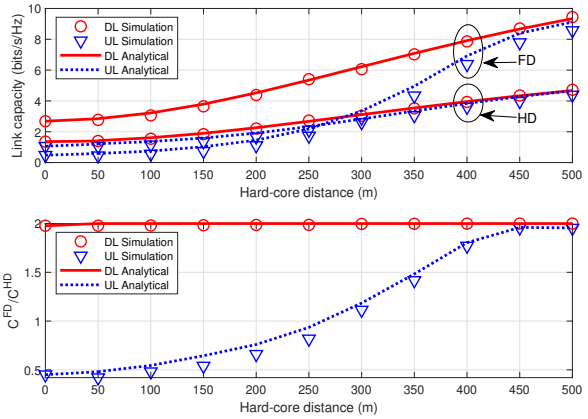

FIGURE 8: Comparison of DL and UL user capacities in FD and HD micro-cellular networks where $l_{k_0^d,B_0}$ and l_{B_0,k_0^u} are given.

and inter-cell interference from BSs become overwhelming when $P_d \gg P_u$. Due to the low outage probability in DL transmission, throughput of DL users is almost constant throughout, while throughput of UL users is increased with hard-core distance. Therefore, UL transmission in FD macro-cellular networks is feasible when a larger hard-core distance between BSs is adopted.

In Fig. 8, we compare the capacities of DL and UL users in FD and HD micro-cell networks for given $l_{k_0^d,B_0}$ and l_{B_0,k_0^u}, $\lambda_P^d = \lambda_P^u = 10.19\ users/km^2$ and $\lambda_{MP} = 5.09\ BS/km^2$. It can be observed that the capacity of DL users in FD micro-cell networks is almost twice that in HD micro-cell networks. This is because for DL transmission, interference from inter-cell BS is dominant and the capacity of a DL user k_0^d can be approximated as $\frac{b_d}{\ln 2}\int_0^\infty \mathcal{L}_{I_{BS}^d}\left(\frac{zG_b\beta P_d}{\sigma^2 l^\alpha_{k_0^d,B_0}}\right)\frac{e^{-z}G_b\beta P_d}{\sigma^2 l^\alpha_{k_0^d,B_0}+zG_b\beta P_d}dz$, which equals $2 \times C^{HD}_{K_0^d|l_{k_0^d,B_0}}$. In the low hard-core distance regime, due to the additional interference from DL BSs in FD networks, HD networks provide better UL link capacity. However, the interference from DL BSs in FD networks is suppressed by

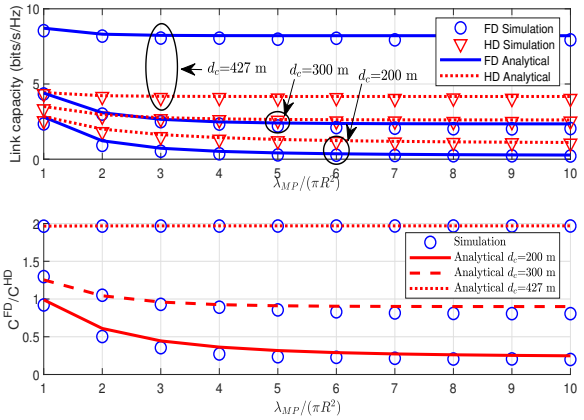

FIGURE 9: Comparison of UL user capacities in FD and HD micro-cellular networks.

increasing hard-core distance, and UL transmission in FD networks outperforms that of HD networks when hard-core distance is large enough.

To further analyze the impacts of hard-core distance and the intensity of candidate BSs on UL transmission, we compare the UL user capacities in FD and HD micro-cellular networks with different hard-core distances in Fig. 9. It can be observed that a suitable hard-core distance between FD BSs should be imposed to make UL transmission feasible in micro-cell networks. Moreover, Fig. 9 shows that the ratio of UL user capacity in FD networks to that in HD networks increases with hard-core distance. And, when hard-core distance is greater than or equal to the critical distance (i.e., $d_c \geq R_c$), UL transmission in FD networks has the potential to double the spectrum efficiency.

VI. CONCLUSION

The performance of a FD cellular network, where a HCPP was used to model the BSs and linear IA was applied at each cell to cancel the intra-cell interference was studied. In addition to providing general expressions for the performance metrics, closed-form approximations of the outage probability and throughput were derived. Simulation and analytical results showed that FD communication is feasible in micro-cellular networks, while large hard-core distances are required to make UL transmission in FD macro-cellular networks a reality. Moreover, results also showed that interference from BSs plays a crucial role in micro-cell systems. When the maximum number of UL users for which IA is feasible is equal to or greater than twice the mean number of UL users in each cell, the residual intra-cell interference from UL users can be ignored. It was clearly seen that even IA is utilized for intra-cell interference management in FD networks, suitable spacing between FD BSs should be imposed to make UL transmission feasible. Moreover, we show that FD networks tend to double the UL user capacity over their HD counterparts when the hard-core distance is greater than or equal to the critical distance.

APPENDIX

A. PROOF OF PROPOSITION 1

$\mathcal{L}_{I^d_{inter}|l_{k_0^d,B_0}}(z)$ can be rewritten as (58).

The PDF of $\| \boldsymbol{u}^H_{k_0^d,t} \boldsymbol{H}_{k_0^d,B_q} \boldsymbol{V}_{i_q^d} \|^2$ has been provided in (8). Therefore, we have

$$\mathbb{E}_{\boldsymbol{H}_{k_0^d,B_q}}\left[e^{-\frac{zl^{\alpha}_{k_0^d,B_0}}{l^{\alpha}_{k_0^d,B_q}}\|\boldsymbol{u}^H_{k_0^d,t}\boldsymbol{H}_{k_0^d,B_q}\boldsymbol{V}_{i_q^d}\|^2}\right] = \left(1+\frac{zl^{\alpha}_{k_0^d,B_0}}{l^{\alpha}_{k_0^d,B_q}}\right)^{-b_d}. \tag{59}$$

Similarly, $2\times \| \boldsymbol{u}^H_{k_0^d,t} \boldsymbol{H}_{k_0^d,j_q^u} \boldsymbol{V}_{j_q^u} \|^2$ is a Chi-squared distributed RV with $2b_u$ DoF and we have

$$\mathbb{E}_{\boldsymbol{H}_{k_0^d,j_q^u}}\left[e^{-\mathcal{S}_d\frac{\beta_u P_u}{l^{\alpha_u}_{k_0^d,j_q^u}}\|\boldsymbol{u}^H_{k_0^d,t}\boldsymbol{H}_{k_0^d,j_q^u}\boldsymbol{V}_{j_q^u}\|^2}\right] = \left(1+\mathcal{S}_d\frac{\beta_u P_u}{l^{\alpha_u}_{k_0^d,j_q^u}}\right)^{-b_u} \tag{60}$$

The coverage probability affected by inter-cell interference can be rewritten as

$$\mathcal{L}_{I^d_{inter}|l_{k_0^d,B_0}}(z) = \mathbb{E}_{\Phi_M}\left[\prod_{B_q\in\Phi_M q\neq 0} G^d_{\varphi}\left(\left(1+\frac{zl^{\alpha}_{k_0^d,B_0}}{l^{\alpha}_{k_0^d,B_q}}\right)^{-b_d}\right) G^d_{\phi}(l,\theta)\right] \tag{61}$$

where the function $G^d_{\varphi}(x)$ is given by

$$G^d_{\varphi}(x) = \mathbb{E}_{\tilde{\varphi}_q}\left[\prod_{i_q^d\in\tilde{\varphi}_q} x\right] = (1-\delta)\mathbb{E}_{\varphi_q}\left[\prod_{i_q^d\in\varphi_q} x\right] + \delta\mathbb{E}_{\varphi'_q}\left[\prod_{i_q^d\in\varphi'_q} x\right] \tag{62}$$

and (19) can be obtained.

$G^d_{\phi}(l,\theta) = \mathbb{E}_{\phi_q}\left[\prod_{j_q^u\in\phi_q}\left(1+\mathcal{S}_d\frac{\beta_u P_u}{l^{\alpha_u}_{k_0^d,j_q^u}}\right)^{-b_u}\right]$, $l_{k_0^d,j_q^u} = \sqrt{l^2_{B_0,j_q^u}+l^2_{k_0^d,B_0}-2l_{B_0,j_q^u}l_{k_0^d,B_0}\cos\left(\theta_{j_q^u}\right)}$, $l_{B_0,j_q^u} = \sqrt{l^2+r^2-2lr\cos(\vartheta)}$ and $\theta_{j_q^u} = \theta - \arcsin\left(\frac{r}{l_{B_0,j_q^u}}\sin(\vartheta)\right)$.

Let $v_1(j_q^u) = \left(1+\mathcal{S}_d\frac{\beta_u P_u}{l^{\alpha_u}_{k_0^d,j_q^u}}\right)^{-b_u}$ and $\forall j_q^u \in \phi_q$, we have $0 \leq v_1(j_q^u) \leq 1$. For ϕ_q, the probability generating function (PGF) is given by

$$G^d_{\phi}(l,\theta) = \exp\left[-\lambda^u_P\int_{R^2}\left(1-v_1(j_q^u)\right)ds\right]. \tag{63}$$

Since the integration area is the circular region centered by B_q with radius R, (20) can be obtained.

To evaluate the expectation in (61), PGF of HCPPs is required. However, it has been reported in the literature that exact PGF of HCPPs does not exist. In [44], it has been proved that the mean interferences at nodes of a MHCPP and a PPP with the same intensity are comparable while the

$$\mathcal{L}_{I^d_{inter}|l_{k_0^d,B_0}}(z) = \mathbb{E}_{\Phi_M}\left\{\prod_{B_q\in\Phi_M\, q\neq 0}\mathbb{E}_{\tilde{\varphi}_q}\left[\prod_{i_q^d\in\tilde{\varphi}_q}\mathbb{E}_{\boldsymbol{H}_{k_0^d,B_q}}\left[\exp\left(-\frac{z l^{\alpha}_{k_0^d,B_0}}{l^{\alpha}_{k_0^d,q}}\parallel \boldsymbol{u}^H_{k_0^d,t}\boldsymbol{H}_{k_0^d,B_q}\boldsymbol{V}_{i_q^d}\parallel^2\right)\right]\right]\right.$$
$$\left.\times\mathbb{E}_{\phi_q}\left[\prod_{j_q^u\in\phi_q}\mathbb{E}_{\boldsymbol{H}_{k_0^d,j_q^u}}\left[\exp\left(-\frac{z l^{\alpha}_{k_0^d,B_0}\beta_u P_u}{l^{\alpha_u}_{k_0^d,j_q^u} G_b\beta P_d}\parallel \boldsymbol{u}^H_{k_0^d,t}\boldsymbol{H}_{k_0^d,j_q^u}\boldsymbol{V}_{j_q^u}\parallel^2\right)\right]\right]\right\} \tag{58}$$

gap never exceeds 1dB. Therefore, we use PGF of PPP to approximate that of MHCPP (this approximation is shown to be tight in simulation section). Assuming $v_2(B_q) = G^d_{\varphi}\left(\left(1+\frac{z l^{\alpha}_{k_0^d,B_0}}{l^{\alpha}_{k_0^d,B_q}}\right)^{-b_d}\right)G^d_{\phi}(l,\theta)$, we have

$$\mathbb{E}\left[\prod_{B_q\in\Phi_M/B_0} v_2(B_q)\right] \approx e^{-\int_0^{2\pi}\int_d^{\infty}\left(1-v_2(B_q)\right)\lambda_M P\rho_M(l) l dl d\theta} \tag{64}$$

where $l_{k_0^d,B_q} = (l^2_{k_0^d,B_0} + l^2 - 2l_{k_0^d,B_0} l\cos(\theta))^{1/2}$, l is the distance from B_q to B_0, and θ is the angle difference of BS B_q and user k_0^d. Due to the exist of hard-core distance between BSs, the value of l varies from d_c to ∞. Substituting the expression for $\rho_M(l)$ into the above equation, the proof of Proposition 1 is complete.

B. PROOF OF COROLLARY 1

Since l is the distance between B_0 and B_q, we have $l \geq d_c$. When $d_c \gg R$, $l \gg l_{k_0^d,B_0}$ and the distance from B_q to k_0^d can be approximated as l. Moreover, when $\delta = 1$ and the intensity of DL users is large enough, we have $G^d_{\varphi}(x) \approx x^{K_d^{max}}$. Therefore, setting $G^d_{\phi}(l,\eta) = 1$ and $\rho_1(l) \approx \rho_2(l)$, (61) can be approximated as

$$\hat{\mathcal{L}}_{I^d_{BS}|l_{k_0^d,B_0}}(\mathcal{S}_d) = e^{-2\pi\lambda_M\int_{d_c}^{\infty}\left(1-\left(1+\frac{A_{bu}}{l^{\alpha}}\right)^{-K_d^{max}b_d}\right)l dl} \tag{65}$$

where $\left(1-\left(1+\frac{A_{bu}}{l^{\alpha}}\right)^{-K_d^{max}b_d}\right)$ can be rewritten as

$$\left(1-\left(1+\frac{A_{bu}}{l^{\alpha}}\right)^{-K_d^{max}b_d}\right) = \sum_{p=0}^{K_d^{max}b_d-1}\binom{p}{K_d^{max}b_d}\frac{A_{bu}^{-p}l^{\alpha p}}{\left(1+\frac{l^{\alpha}}{A_{bu}}\right)^{K_d^{max}b_d}}. \tag{66}$$

Letting $t = l^{\alpha}$, we have $l = t^{1/\alpha}$, $dl = \frac{1}{\alpha}t^{1/\alpha-1}dt$ and

$$\hat{\mathcal{L}}_{I^d_{BS}|l_{k_0^d,B_0}}(\mathcal{S}_d) = \exp\left(-2\pi\lambda_M\sum_{p=0}^{K_d^{max}b_d-1}\binom{p}{K_d^{max}b_d}\right.$$
$$\left.\times\int_{(d_c)^{\alpha}}^{\infty}\frac{A_{bu}^{-p}t^{p+2/\alpha-1}}{\alpha\left(1+\frac{1}{A_{bu}}t\right)^{K_d^{max}b_d}}dt\right). \tag{67}$$

Finally, applying [42, 3.194.2] (25) is obtained, proving Corollary 1.

C. PROOF OF PROPOSITION 2

When $\delta = 0$, we have $\mathcal{L}_{I^d_{RUL}}(\mathcal{S}_d) = 1$. For the second case, distance from the K_u^{max}th nearest UL user to B_0 is denoted as $r_{K_u^{max}}$. All the intra-cell interference from UL users can be cancelled when $r_{K_u^{max}} \geq R$. Given $r_{K_u^{max}}$ ($r_{K_u^{max}} < R$), the UL users distributed in the ring with radius $r_{K_u^{max}} \leq r \leq R$ and centered by B_0 form a subset of PPP ϕ_0', since they are randomly distributed in the ring and their number is Poisson distributed. Thus, $\mathcal{L}_{I^d_{RUL}}(z)$ can be written as (68). Following steps similar to the proof of Proposition 1, $\mathcal{L}_{I^d_{RUL}}(z)$ can be rewritten as

$$\mathcal{L}_{I^d_{RUL}|l_{k_0^d,B_0}}(\mathcal{S}_d) = 1-\delta+\delta\left\{\sum_{K_u=0}^{K_u^{max}-1}P(K_u)\right.$$
$$\left.+\int_0^R f_{K_u^{max}}(r)\mathbb{E}_{\phi_0'}\left[\prod_{j_0^u\in\phi_0'}\left(1+\frac{A_{uu}}{l^{\alpha}_{k_0^d,j_0^u}}\right)^{-b_u}\right]dr\right\} \tag{69}$$

where the expectation can be obtained as

$$\mathbb{E}_{\phi_0'}\left[\prod_{j_0^u\in\phi_0'}\left(1+\frac{A_{uu}}{l^{\alpha}_{k_0^d,j_0^u}}\right)^{-b_u}\right]$$
$$= \exp\left[-\lambda_P^u\int_0^{2\pi}\int_{r_{K_u^{max}}}^R\left(1-\left(1+\frac{A_{uu}}{l^{\alpha}_{k_0^d,j_0^u}}\right)^{-b_u}\right)l dl d\theta\right]. \tag{70}$$

This completes the proof of Proposition 2.

D. PROOF OF PROPOSITION 3

Since the elements of $\hat{\boldsymbol{H}}_{B_0,B_0}$ are i.i.d. RVs with distribution $\mathcal{CN}(0,\sigma_s^2)$. Thus, $\frac{2}{\sigma_s^2}\parallel \boldsymbol{u}^H_{k_0^u,t}\hat{\boldsymbol{H}}_{B_0,B_0}\boldsymbol{V}_{i_0^d}\parallel^2$ is a Chi-squared distributed RV with $2b_d$ DoF and its PDF can be written as

$$f_{\chi^2}\left(\frac{2}{\sigma_s^2}x;2b_d\right) = \frac{x^{b_d-1}}{2\sigma_s^{2(b_d-1)}\Gamma(b_d)}e^{-\frac{x}{\sigma_s^2}}. \tag{71}$$

The expression for $\mathcal{L}_{I_{SI}|l_{B_0,k_0^u}}(\mathcal{S}_u)$ can be obtained as

$$\mathcal{L}_{I_{SI}|l_{B_0,k_0^u}}(\mathcal{S}_u)$$
$$= \mathbb{E}_{\tilde{\varphi}_0}\left\{\prod_{i_0^d\in\tilde{\varphi}_0}\int_0^{\infty}f_{\chi^2}(\frac{2}{\sigma_s^2}x;2b_d)e^{-\mathcal{S}_u G_b^2\beta_{b_1}P_d x}d\left(\frac{2}{\sigma_s^2}x\right)\right\}$$
$$= \mathbb{E}_{\tilde{\varphi}_0}\left\{\prod_{i_0^d\in\tilde{\varphi}_0}\left(1+\mathcal{S}_u G_b^2\beta_{b_1}P_d\sigma_s^2\right)^{-b_d}\right\} \tag{72}$$

$$\mathcal{L}_{I^d_{RUL}|l_{k^d_0,B_0}}(\mathcal{S}_d) = 1-\delta+\delta\left\{\int_R^{\infty} f_{K_u^{max}}(r)dr + \int_0^R f_{K_u^{max}}(r)\,\mathbb{E}_{I^d_{RUL}}\left[e^{-\mathcal{S}_d\sum_{j^u_0\in\phi'_0}\frac{\beta_u P_u}{l^{\alpha_u}_{k^d_0,j^u_0}}\|\boldsymbol{u}^H_{k^d_0,t}\boldsymbol{H}_{k^d_0,j^u_0}\boldsymbol{V}_{j^u_0}\|^2}\right]dr\right\} \tag{68}$$

Solving the above expectation, the proof of Proposition 3 is obtained.

REFERENCES

[1] A. Sabharwal, P. Schniter, D. Guo, D. W. Bliss, S. Rangarajan, and R. Wichman, "In-band full-duplex wireless: Challenges and opportunities," IEEE Journal on Selected Areas in Communications, vol. 32, no. 9, pp. 1637–1652, 2014.

[2] P. Aquilina, A. C. Cirik, and T. Ratnarajah, "Weighted sum rate maximization in full-duplex multi-user multi-cell mimo networks," IEEE Transactions on Communications, vol. 65, no. 4, pp. 1590–1608, 2017.

[3] A. C. Cirik, S. Biswas, S. Vuppala, and T. Ratnarajah, "Beamforming design for full-duplex mimo interference channels–qos and energy-efficiency considerations," IEEE Transactions on Communications, vol. 64, no. 11, pp. 4635–4651, 2016.

[4] D. Korpi, T. Riihonen, V. Syrjälä, L. Anttila, M. Valkama, and R. Wichman, "Full-duplex transceiver system calculations: Analysis of ADC and linearity challenges," IEEE Transactions on Wireless Communications, vol. 13, no. 7, pp. 3821–3836, 2014.

[5] M. Duarte and A. Sabharwal, "Full-duplex wireless communications using off-the-shelf radios: Feasibility and first results," in Signals, Systems and Computers (ASILOMAR), 2010 Conference Record of the Forty Fourth Asilomar Conference on. IEEE, 2010, pp. 1558–1562.

[6] D. Bharadia, E. McMilin, and S. Katti, "Full duplex radios," ACM SIGCOMM Computer Communication Review, vol. 43, no. 4, pp. 375–386, 2013.

[7] M. Amjad, F. Akhtar, M. H. Rehmani, M. Reisslein, and T. Umer, "Full-duplex communication in cognitive radio networks: A survey," IEEE Communications Surveys & Tutorials, vol. 19, no. 4, pp. 2158–2191, 2017.

[8] L. Qiang, S. Feng, X. Ge, G. Mao, and L. Hanzo, "Outage performance of full-duplex multi-relay channels with relay selection," IEEE Transactions on Vehicular Technology, vol. PP, no. 99, pp. 9550–9554, 2017.

[9] C. Psomas, M. Mohammadi, I. Krikidis, and H. A. Suraweera, "Impact of directionality on interference mitigation in full-duplex cellular networks," IEEE Transactions on Wireless Communications, vol. 16, no. 1, pp. 487–502, 2017.

[10] Z. Zhang, X. Chai, K. Long, A. V. Vasilakos, and L. Hanzo, "Full duplex techniques for 5g networks: self-interference cancellation, protocol design, and relay selection," IEEE Communications Magazine, vol. 53, no. 5, pp. 128–137, May, 2015.

[11] D. Kim, H. Lee, and D. Hong, "A survey of in-band full-duplex transmission: From the perspective of phy and mac layers," IEEE Communications Surveys & Tutorials, vol. 17, no. 4, pp. 2017–2046, 2017.

[12] H. Ju, D. Kim, H. V. Poor, and D. Hong, "Bi-directional beamforming and its capacity scaling in pairwise two-way communications," IEEE Transactions on Wireless Communications, vol. 11, no. 1, pp. 346–357.

[13] S. Kam, D. Kim, H. Lee, and D. Hong, "Bi-directional full-duplex systems in a multi-spectrum environment," IEEE Transactions on Vehicular Technology, vol. 64, no. 8, p. 3812–3817, Aug, 2015.

[14] H. Ju, E. Oh, and D. Hong, "Catching resource-devouring worms in next-generation wireless relay systems: Two-way relay and full-duplex relay," IEEE Communications Magazine, vol. 47, no. 9, pp. 58–65, 2009.

[15] R. Li, Y. Chen, G. Y. Li, and G. Liu, "Full-duplex cellular networks," IEEE Communications Magazine, vol. 55, no. 4, pp. 184–191, 2017.

[16] J. Bai and A. Sabharwal, "Asymptotic analysis of mimo multi-cell full-duplex networks," IEEE Transactions on Wireless Communications, vol. 16, no. 4, pp. 2168–2180, 2017.

[17] L. Haesoon, P. Yosub, and H. Daesik, "Resource split full duplex to mitigate inter-cell interference in ultra-dense small cell networks," IEEE Access, vol. 6.

[18] R. K. Mungara, I. Thibault, and A. Lozano, "Full-duplex MIMO in cellular networks: System-level performance," IEEE Transactions on Wireless Communications, vol. 16, no. 5, pp. 3124–3137, 2017.

[19] Z. Tong and M. Haenggi, "Throughput analysis for wireless networks with full-duplex radios," in 2015 IEEE Wireless Communications and Networking Conference (WCNC). IEEE, 2015, pp. 717–722.

[20] J. Lee and T. Q. Quek, "Hybrid full-/half-duplex system analysis in heterogeneous wireless networks," IEEE transactions on wireless communications, vol. 14, no. 5, pp. 2883–2895, 2015.

[21] H. He, J. Xue, T. Ratnarajah, F. A. Khan, and C. B. Papadias, "Modeling and analysis of cloud radio access networks using matérn hard-core point processes," IEEE Transactions on Wireless Communications, vol. 15, no. 6, pp. 4074–4087, 2016.

[22] A. Guo and M. Haenggi, "Spatial stochastic models and metrics for the structure of base stations in cellular networks," IEEE Transactions on Wireless Communications, vol. 12, no. 11, pp. 5800–5812, 2013.

[23] V. R. Cadambe and S. A. Jafar, "Interference alignment and degrees of freedom of the k-user interference channel," IEEE Transactions on Information Theory, vol. 54, no. 8, pp. 3425–3441, 2008.

[24] K. Gomadam, V. R. Cadambe, and S. A. Jafar, "A distributed numerical approach to interference alignment and applications to wireless interference networks," IEEE Transactions on Information Theory, vol. 57, no. 6, pp. 3309–3322, 2011.

[25] D. A. Schmidt, C. Shi, R. A. Berry, M. L. Honig, and W. Utschick, "Minimum mean squared error interference alignment," in 2009 Conference Record of the Forty-Third Asilomar Conference on Signals, Systems and Computers. IEEE, 2009, pp. 1106–1110.

[26] J. Bai, S. Diggavi, and A. Sabharwal, "On degrees-of-freedom of multi-user MIMO full-duplex network," in IEEE International Symposium on Information Theory (ISIT), June 2015, pp. 864–868.

[27] K. Kim, S.-W. Jeon, and D. K. Kim, "The feasibility of interference alignment for full-duplex MIMO cellular networks," IEEE Communications Letters, vol. 19, no. 9, pp. 1500–1503, 2015.

[28] P. Aquilina and T. Ratnarajah, "Linear interference alignment in full-duplex MIMO networks with imperfect CSI," IEEE Transactions on Communications, vol. 65, no. 12, pp. 5226–5243, Dec. 2017.

[29] M. A. A. Khojastepour, K. Sundaresan, S. Rangarajan, and M. Farajzadeh-Tehrani, "Scaling wireless full-duplex in multi-cell networks," in 2015 IEEE Conference on Computer Communications (INFOCOM), 2015, pp. 1751–1759.

[30] I. Randrianantenaina, H. ElSawy, H. Dahrouj, M. Kaneko, and M.-S. Alouini, "Uplink power control and ergodic rate characterization in fd cellular networks: A stochastic geometry approach," IEEE Transactions on Wireless Communications, vol. 18, no. 4, p. 2093–2110, 2019.

[31] A. Sadeghi, M. Luvisotto, F. Lahouti, S. Vitturi, and M. Zorzi, "Statistical qos analysis of full duplex and half duplex heterogeneous cellular networks," in 2016 IEEE International Conference on Communications, 2016, pp. 1–6.

[32] I. Atzeni, M. Kountouris, and G. C. Alexandropoulos, "Performance evaluation of user scheduling for full-duplex small cells in ultra-dense networks," pp. 1–6, 2016.

[33] H. He, P. Aquilina, and T. Ratnarajah, "Full-duplex multi-cell networks with interference alignment," in 2019 IEEE 16th International Symposium on Wireless Communication Systems (ISWCS), pp. 91–95.

[34] C. Saha, M. Afshang, and H. S. Dhillon, "Enriched k -tier hetnet model to enable the analysis of user-centric small cell deployments," IEEE Transactions on Wireless Communications, vol. 16, no. 3, pp. 1593–1608, 2017.

[35] T. K. Sarkar, Z. Ji, K. Kim, A. Medouri, and M. Salazar-Palma, "A survey of various propagation models for mobile communication," IEEE Antennas and propagation Magazine, vol. 45, no. 3, pp. 51–82, 2003.

[36] R. K. Mungara and A. Lozano, "Interference surge in full-duplex wireless systems," in Signals, Systems and Computers, 2015 49th Asilomar Conference on. IEEE, 2015, pp. 25–29.

[37] T. Riihonen, S. Werner, and R. Wichman, "Hybrid full-duplex/half-duplex relaying with transmit power adaptation," IEEE Transactions on Wireless Communications, vol. 10, no. 9, pp. 3074–3085, 2011.

[38] K. A. Hamdi, "A useful lemma for capacity analysis of fading interference channels," IEEE Transactions on Communications, vol. 58, no. 2, 2010.

[39] R. Vaze and R. W. Heath, "Transmission capacity of ad-hoc networks with multiple antennas using transmit stream adaptation and interference cancellation," IEEE Transactions on Information theory, vol. 58, no. 2, pp. 780–792, 2012.

[40] S. N. Chiu, D. Stoyan, W. S. Kendall, and J. Mecke, Stochastic geometry and its applications. John Wiley & Sons, 2013.
[41] A. Al-Hourani, R. J. Evans, and S. Kandeepan, "Nearest neighbor distance distribution in hard-core point processes," IEEE Communications Letters, vol. 20, no. 9, pp. 1872–1875, 2016.
[42] I. S. Gradshteyn and I. M. Ryzhik, Table of integrals, series, and products. Academic press, 2014.
[43] M. Haenggi, "On distances in uniformly random networks," IEEE Transactions on Information Theory, vol. 51, no. 10, pp. 3584–3586, 2005.
[44] ——, "Mean interference in hard-core wireless networks," IEEE Communications Letters, vol. 15, no. 8, pp. 792–794, 2011.

HUASEN HE received the B.S. degree in Automation from University of Science and Technology of China, Hefei, China, in 2013, and the M.S. degree in Signal Processing and Communications in 2014, Ph.D. degree in Digital Communications in 2018, both from the University of Edinburgh, Edinburgh, U.K. He is currently an associate research fellow with the School of Information Science and Technology, USTC. His research interests include space-terrestrial integrated network, stochastic geometry, future network architecture and signal processing for communication.

SUDIP BISWAS (S'16-M'20) received the Ph.D. degree in Digital Communications in 2017 from the University of Edinburgh (UEDIN), UK and currently works at the Indian Institute of Information Technology Guwahati (IIITG) as an Asst. Professor in the Department of Electronics and Communications Engineering. He leads research in signal processing for wireless communications, with particular focus on 5G's long-term evolution, including transceiver design for full-duplex radios, wireless edge caching, comms-radar co-existence and large intelligent surface assisted communication. Prior to this he held the position of Research Associate from 2017 to 2019 at the Institute of Digital Communications in UEDIN. He also has industrial experience with Tata Consultancy Services, India (Lucknow & Kolkata), where he held the position of Asst. Systems Engineer from 2010 to 2012. He was an organizer of the IEEE International Workshop on Signal Processing Advances in Wireless Communications (SPAWC), Edinburgh, UK, 2016 and has been involved in EU FP7 projects: remote radio heads & parasitic antenna arrays (HARP) and dynamic licensed shared access (ADEL), a DST UKIERI project on wireless edge caching and an EPSRC project on NoMA.

PAULA AQUILINA (S'14) received the B.Eng. (Hons.) degree in electrical engineering from the University of Malta in 2010, and the M.Sc. degree in signal processing and communications and the Ph.D. degree in engineering (digital communications) from The University of Edinburgh in 2013 and 2017, respectively. Her main area of research is wireless communications, with particular focus on interference management and network information theory.

THARMALINGAM RATNARAJAH (Senior Member, IEEE) is currently with the Institute for Digital Communications, The University of Edinburgh, Edinburgh, U.K., as a Professor in digital communications and signal processing. He has supervised 15 Ph.D. students and 21 postdoctoral research fellows and raised more than 11+ million USD of research funding. He was the Coordinator of the EU projects ADEL (3.7M€) in the area of licensed shared access for 5G wireless networks, HARP (4.6M€) in the area of highly distributed MIMO, the EU Future and Emerging Technologies projects HIATUS (3.6M€) in the area of interference alignment, and CROWN (3.4M€) in the area of cognitive radio networks. His research interests include signal processing and information theoretic aspects of 5G and beyond wireless networks, full-duplex radio, mmWave communications, random matrix theory, statistical and array signal processing, and quantum information theory. He has published over 400 articles in these areas and holds four U.S. patents. He is a Fellow of the Higher Education Academy (FHEA). He was an Associate Editor of the IEEE TRANSACTIONS ON SIGNAL PROCESSING, from 2015 to 2017, and the Technical Co-Chair in the 17th IEEE International Workshop on Signal Processing Advances in Wireless Communications, Edinburgh, in 2016.

JIAN YANG received the B.S. and Ph.D. degrees from the University of Science and Technology of China (USTC), Hefei, China, in 2001 and 2006, respectively. From 2006 to 2008, he was a Post-Doctoral Scholar with the Department of Electronic Engineering and Information Science, USTC. Since 2008, he has been an Associate Professor with the Department of Automation, USTC.,He is currently a Professor with the School of Information Science and Technology, USTC. His research interests include future network, distributed system design, modeling and optimization, multimedia over wired and wireless networks, and stochastic optimization. He received the Lu Jia-Xi Young Talent Award from the Chinese Academy of Sciences in 2009. (Based on document published on 28 November 2018).